Estrogen Receptor β Deficiency Impairs Gut Microbiota: A Possible Mechanism for IBD-Related Anxiety-Like Behavior

Yuanyuan Ma
Third Military Medical University: Army Medical University
Tianyao Liu
Third Military Medical University: Army Medical University
Xin Li
Third Military Medical University: Army Medical University
Anqi Kong
Soochow University
Rui Xiao
Third Military Medical University: Army Medical University
Ruxin Xie
Third Military Medical University: Army Medical University
Junwei Gao
Third Military Medical University: Army Medical University
Zhongke Wang
Third Military Medical University: Army Medical University
Yun Cai
Third Military Medical University: Army Medical University
Jiao Zou
Third Military Medical University: Army Medical University
Ling Yang
Third Military Medical University: Army Medical University
Lian Wang
Third Military Medical University: Army Medical University
Jinghui Zhao
Third Military Medical University: Army Medical University
Haiwei Xu
Third Military Medical University Southwest Hospital
Warner Margaret
Karolinska Institute: Karolinska Institutet
Xingshun Xu

Soochow University

Jan-Ake Gustafsson

Karolinska Institute: Karolinska Institutet

Xiaotang Fan (fanxiaotang2005@163.com)

Third Military Medical University: Army Medical University https://orcid.org/0000-0001-5694-1828

Research

Keywords: anxiety, ErbB4, estrogen receptor β, gut microbiota, hypothalamic-pituitary-adrenal axis, inflammatory bowel disease, stress

Posted Date: October 20th, 2021

DOI: https://doi.org/10.21203/rs.3.rs-956243/v1

Estrogen receptor β deficiency impairs gut microbiota: a possible mechanism for IBD-induced anxiety-like behavior

Yuanyuan Ma[a,#], Tianyao Liu[a,#], Xin Li[a], Anqi Kong[b], Rui Xiao[a], Ruxin Xie[a], Junwei Gao[a], Zhongke Wang[a], Yun Cai[a], Jiao Zou[a], Ling Yang[a], Lian Wang[a], Jinghui Zhao[a], Haiwei Xu[c], Warner Margaret[d], Xingshun Xu[b,*], Jan-Ake Gustafsson[d,e,*], Xiaotang Fan[a,*]

[a]Department of Military Cognitive Psychology, School of Psychology, Third Military Medical University, Chongqing, China

[b]Institute of Neuroscience, Soochow University, Suzhou, China

[c]Southwest Eye Hospital, Southwest Hospital, Third Military Medical University, Chongqing, China

[d]Center for Innovative Medicine, Department of Biosciences and Nutrition, Karolinska Institute, Stockholm, Sweden

[e]Center for Nuclear Receptors and Cell Signaling, University of Houston, Houston, USA

[#]The authors contributed equally to this work.

[*]To whom correspondence should be addressed. E-mail: xingshunxu@suda.edu.cn, jgustafsson@uh.edu or fanxiaotang2005@163.com

Short title: ERβ-induced microbiota in IBD-related anxiety.

Grant support: This work was supported by the National Key R&D Program of China (2017YFE0103700), and National Nature Science Foundation of China (No. 31871043).

Disclosure: The authors declare that they have no conflict of interests.

Abstract

Although lack of ERβ is an acknowledged risk factor for the development of inflammatory bowel disease (IBD) and psychiatric disorders, the underlying cellular and molecular mechanisms are not fully understood. Here, we showed that ERβ knockout mice upon dextran sodium sulfate (DSS) insult displayed significant shifts in fecal microbiota composition (enrichment of *Prevotellaceae_UCG_001*), aggravated colitis severity and anxiety-like behaviors, but not depression-like behavior. In addition, DSS induced colitis also enhanced hypothalamic-pituitary-adrenal (HPA) axis hyperactivity in ERβ-deficiency mice, which linked colitis and anxiety-like behaviors. In line with these observations, RNA sequencing data further identified ErbB4 might be the target of ERβ involved in regulating HPA axis hyperactivity caused by DSS insult. Gut microbiota remodeling by co-housing showed both colitis severity and anxiety-like behaviors were aggravated in co-housed WT mice compared with single-housed WT mice, suggesting that gut microbiota plays a critical role in mediating colitis disease activity and related anxiety-like behaviors via aberrant neural processing within the gut-brain axis. Our findings demonstrate ERβ has the potential to inhibit colitis development and anxiety-like behaviors via remodeling of the gut microbiota, which reveals ERβ as a promising therapeutic target for treating IBD and related anxiety-like behaviors.

Key words: anxiety, ErbB4, estrogen receptor β, gut microbiota, hypothalamic-pituitary-adrenal axis, inflammatory bowel disease, stress

Introduction

Inflammatory bowel disease (IBD), including Crohn's disease and ulcerative colitis, is a group of chronic disabling disease that causes gastrointestinal tract symptoms [1]. Psychiatric comorbidities such as anxiety and depression are frequently occurred in IBD patients, with up to a third of patients affected by anxiety symptoms and a quarter affected by depression symptoms, which bring a great challenge for patients including the physiological and psychological health care [2, 3]. Indeed, psychiatric symptoms appear to be more prevalent during active disease states of IBD [4], which has been regarded as a disorder of gut-brain communication, but the mechanisms behind it are less clearly understood.

Abnormal gut microbiota profiles, referred as gut dysbiosis, influencing host physiology through gut barrier homeostasis and gut inflammation, is one of major pathogenic factors in the development of IBD [5]. An increasing amount of evidences have shown that gut dysbiosis are more frequently reported IBD patients [6, 7]. Remarkably, it has been confirmed that gut dysbiosis is correlated with a wide range of mental health conditions, such as anxiety and depression via the microbiota-gut-brain axis. Mice receiving irritable bowel syndrome fecal microbiota showed faster gut motility, gut barrier dysfunction, colon inflammation activation and anxiety-like behavior [8]. Kilinçarslan et al. [9] also indicated that fecal microbiota transplantation alleviated the severity of anxiety, depression and obsession as well as gastrointestinal symptoms in IBD patients. It was further revealed that the use of microbiota manipulation such as prebiotics and probiotics can improve gut abnormality and neurobehavior deficits [10, 11]. Therefore, gut dysbiosis is closely linked to gut dysfunctions and related mood disorders in gastrointestinal diseases.

The composition of gut microbiota remains relatively constant throughout adult life, and it will be altered under different circumstances that subsequently influence the host's health status [12]. Nevertheless, there are strong evidences indicated that even variation of one single host gene can significantly alter the host-microbe interactions [13]. Estrogen receptor (ER) β is the predominant ER subtype in colon tissue and plays an important role in colonic mucosal homeostasis by maintaining the integrity of tight junctions and barrier function in the colon [14, 15]. It has been confirmed that the expression of ERβ is markedly reduced in active ulcerative colitis and Crohn's disease patients [15, 16], implicating essential role of ERβ in the development of IBD. Intriguingly, it's reported that sex hormones including testosterone and estradiol are correlated with the changes of gut microbiota composition in human [17]. It has been further supported by the evidence that intestinal epithelial cell-specific deletion of ERβ can alter the gut microbiota composition in mice [18]. Additionally, accumulating studies demonstrated that ERβ could exert anxiolytic effects in rodents. Selective ERβ agonists can reduce anxiety-like behaviors in mice [19]. It seemed that ERβ is important in maintaining gut homeostasis and mental health condition. However, the underlying mechanisms that ERβ drives microbiota mediated development of IBD as well as altered behaviors remain to be demonstrated.

In this study, we found that ERβ knockout ($ER\beta^{-/-}$) mice with acute colitis induced by dextran sulfate sodium (DSS) exhibited anxiety-like behavior. Meanwhile, ERβ deficiency in mice caused alterations of gut microbiota composition and increased the susceptibility of colitis. Hypothalamic-pituitary-adrenal (HPA) axis hyperactivity rather than neuroinflammation is involved in this IBD-related anxiety-like disorders when loss of ERβ in mice. Cohousing WT mice with $ER\beta^{-/-}$ mice further showed the perturbed gut microbiota

which was the real mechanism behind the IBD-related anxiety-like performance. Our findings highlight that gut microbiota acts as a triggering event in IBD and related anxiety-like behavior in ERβ-deficiency mice.

Materials and methods

Mice

Mice were housed in a specific-pathogen-free facility of the Third Military Medical University and got ad libitum access to standard mouse chow and water in a controlled condition under a 12-h light-dark cycle. The experimental procedures were carried out in line with the Guidelines for Animal Committee of Third Military Medical University. $ER\beta^{-/-}$ mice were generated by crossing $ER\beta^{+/-}$ male with female mice [20]. Transgenic mice were backcrossed with C57BL/6 mice for at least seven generations. The sample sizes for all animal experiments are indicated in each figure legend.

DSS colitis model

Acute colitis was induced in 9-10 weeks old male mice by adding 2% dextran sulfate sodium (DSS) (36,000-50,000 M.Wt, MP Biomedicals) in the drinking water for 5 days. At day 5 after exposure to DSS, mice were sacrificed under anaesthesia, and colon and brain tissues were removed and assessed for histological analysis. Partial DSS-treated mice were then allowed to recover by drinking normal water for additional 5 days. Severity of colitis was determined by weight loss, rectal bleeding, and diarrhea daily. Scores are defined as follows [21]: stool bleeding: 0=normal, 1=red, 2=dark red, 3=gross bleeding; stool consistency: 0=normal, 1=soft, 2=very soft, 3=diarrhea.

Co-housing experiment

For co-housing experiments, 4-week old sex-matched WT and ERβ$^{-/-}$ mice originating from the same breeders were divided for either single-housed (SiHo) or co-housed (CoHo) for 6 weeks. CoHo mice were compared to their SiHo littermates as controls. After co-housing, mice were administered with 2% DSS, and explored the severity of colitis and anxiety-like behaviors of SiHo and CoHo WT and ERβ$^{-/-}$ mice later.

Statistical analysis

Data were analyzed by the Statistical Package for the Social Sciences version 25.0 for Windows (SPSS Inc). Data were assessed for normal distribution and plotted in the figures as mean ± SEM or box-plots. Two-way ANOVA with Boferroni's *post hoc* test was used for comparisons with two variables. Relative abundances of specific bacteria among groups were tested using non-parametric Wilcoxon rank sum. For all statistical comparisons, **P*<0.05, ***P*<0.01, and ****P*<0.001.

Detailed methods are described in the Supplementary materials and methods.

Results

DSS-induced colitis led to anxiety- but not depression-like behaviors in ERβ$^{-/-}$ mice

A growing body of evidence has indicated that anxiety- and depression-like behaviors are imperative co-morbidities in IBD, but the link between ERβ and IBD-induced mood behavior deficits remains correlative at present. [22]. To determine whether the DSS-induced colitis affected these behaviors, both ERβ$^{-/-}$ and WT male mice were treated with 2% DSS in drinking water for 5 days, then subjected to a panel of behavioral tests. In the open field test, all groups of mice showed similar locomotor activity (total distance traveled) (Fig. 1A, B). However, DSS-treated ERβ$^{-/-}$ mice exhibited reduced time (Fig. 1C) and

frequency in the center area (Fig. 1D) than control ERβ$^{-/-}$ and DSS-treated WT mice in the open field test, indicating that DSS treatment increased anxiety-like behaviors in ERβ$^{-/-}$ mice. In the elevated plus maze test, DSS-treated ERβ$^{-/-}$ mice spent significantly less time in the open arms and entered the open arms less frequently than control ERβ$^{-/-}$ mice (Fig. 1F, G). Meanwhile, there were also obvious differences in the time spent in the open arms between DSS-treated WT and ERβ$^{-/-}$ mice (Fig. 1F). This assay supported the notion that loss of ERβ leads to an increase in anxiety-like behavior following treated with DSS. In the light-dark box test, DSS-treated ERβ$^{-/-}$ mice spent significantly more time exploring in the dark chamber than both control ERβ$^{-/-}$ and DSS-treated WT mice (Fig. 1H, I). However, no difference in the transition frequencies between light and dark chambers among 4 groups was observed (Fig. 1J). The tail suspension test and forced swimming test were conducted to explore the depression-like behaviors in mice. In these two assays, mice among 4 groups showed indistinguishable immobility time (Fig. 1K, L), indicative of no significant depressive behaviors in these mice. In the nest building, Y maze, novel object recognition test and three chamber test, there were no significant differences between WT and ERβ$^{-/-}$ mice treated with DSS, suggesting that ERβ deficiency might not influence the sensorimotor function, memory function, and social interactions in mice following DSS treatment (Fig. S1). Collectively, these data suggested an involvement of ERβ in conferring resilience to anxiety in a variety of anxiogenic situations when mice were suffering from colitis.

ERβ deficiency resulted in a shifted microbiota composition

Recent studies have confirmed that changes in the gut microbiota are often closely associated with anxiety disorders [23, 24]. To reveal whether gut microbiota is involved in

the anxiety-like behaviors in DSS treated ERβ$^{-/-}$ mice, the fecal microbiota composition were analyzed using MiSeq 16S rRNA gene sequencing. ERβ deficiency led to a reduction in community richness in homeostasis status, as shown in observed OTUs (Fig. 2A), suggesting that the gut microbiota of ERβ$^{-/-}$ mice had less species variation compared to WT mice. While after DSS, the observed OTUs were increased in DSS-treated ERβ$^{-/-}$ mice than that in control ERβ$^{-/-}$ mice (Fig. 2A). PCoA revealed clearly separate clusters for ERβ$^{-/-}$ and WT male mice under homeostasis status or treated with DSS (Fig. 2B).

ERβ deletion in mice dramatically altered the composition of gut microbiota (Fig. 2C-E). Comparative analysis was performed to identify the taxa with significantly altered relative abundance at various ranks. Compared to WT mice, ERβ$^{-/-}$ male mice had higher abundance of bacteria belonging to the genus *Bacteroides*, *Prevotellaceae_UCG_001* and *Quinella* (Fig. 2F). At the family level, significantly higher proportion of *Veillonellaceae* was observed in ERβ$^{-/-}$ mice compared with WT mice (Fig. 2G). ERβ$^{-/-}$ mice also showed enrichments in class *Bacteroidia*, *Campylobacteria* and *Negativicutes*, and order *Bacteroidales* and *Campylobacterales* compared with WT mice (Fig. S2). Compared with control WT mice, DSS-treated WT mice exhibited higher levels of genus *Bacteroides* and *Prevotellaceae_UCG_001*, as well as family *Bacteroidaceae* (Fig. 2F, G). DSS-treated ERβ$^{-/-}$ mice showed higher abundance of *Bacteroides* and *Prevotellaceae_UCG_001* in genus level compared to control ERβ$^{-/-}$ mice (Fig. 2F, G). The relative abundance of genus *Prevotellaceae_UCG_001* was higher in ERβ$^{-/-}$ mice than that in WT mice after treated with DSS, and there was an upward trend in family *Prevotellaceae* of DSS-treated ERβ$^{-/-}$ mice compared to DSS-treated WT mice (Fig. 2F, G). Overall, these data showed that ERβ deficiency induced a shifted gut microbiota composition under either basal or inflammatory

status.

ERβ deficiency aggravated the development of DSS-induced colitis in male mice.

The gut function and inflammatory responses act as important mediators between the gut microbiota and brain [25, 26]. To evaluate the role of ERβ in the colitis pathogenesis, the body weight, rectal bleeding and stool consistency were monitored for 10 days. After administration of DSS for 5 days, the body weight of ERβ$^{-/-}$ mice steadily decreased, and ERβ$^{-/-}$ mice had lost 13.1% of their initial body weight by day 8 (Fig. 3A). In contrast, WT mice exhibited minimal body weight loss and recovered body weight quickly when fed with normal drinking water (Fig. 3A). Similarly, ERβ$^{-/-}$ mice suffered from significant rectal bleeding (Fig. 3B) and diarrhea (Fig. 3C).

We next examined histological features of colonic tissues with hematoxylin and eosin (HE), alcian-blue periodic acid schiff (AB-PAS) and Claudin1 staining. Although ERβ$^{-/-}$ and WT control mice exhibited comparable histological features (Fig. 3D, Fig. S3), more severe colonic ulceration, crypt damage and inflammation were observed in DSS-treated ERβ$^{-/-}$ mice compared with DSS-treated WT mice on day 5 (Fig. 3D, E, Fig. S3), suggesting that ERβ plays a pivotal role in maintaining colonic epithelial homeostasis under DSS induced gut inflammation status. Colonic lengths are comparable between genotypes under normal conditions, while on day 5 post-DSS initiation, the colon length of ERβ$^{-/-}$ mice was significantly shortened than that in WT mice (Fig. 2F).

Macrophage infiltration and higher levels of pro-inflammatory factors determine the colonic inflammation of IBD. Immunofluorescence staining showed an increase of infiltrated macrophages (F4/80^{+}) in the colon of DSS-treated ERβ$^{-/-}$ mice compared with DSS-treated WT mice on day 5 (Fig. S4). We also detected dramatically increased mRNA

levels of pro-inflammatory cytokine genes in the colon of ERβ$^{-/-}$ mice 5 days post-DSS, including *Tnfa*, *Il1b*, *Il6*, *Il17a*, *Cxcl1* and *Ifng* (Fig. 3G). Collectively, these results indicated that ERβ$^{-/-}$ mice displayed deficiency of colonic epithelium, severe colonic inflammation and robust colitis after DSS treatment.

Hypothalamic-pituitary-adrenal (HPA) axis was dysregulated in ERβ$^{-/-}$ mice with DSS-induced colitis.

Studies indicated that dysbiosis or gut inflammation might induce neurological disorders via neuroinflammation or HPA axis [23, 27-30]. To confirm whether neuroinflammation elicited by loss of ERβ is involved in the gut-brain communications, the number of microglia in brain regions related to anxiety-like behavior was evaluated. There was no significant difference in the number of ionized calcium binding adapter molecule 1 (Iba1) positive cells between DSS-treated WT and ERβ$^{-/-}$ mice in mPFC, amygdala and ventral hippocampus 5 days post-DSS (Fig. S5).

The HPA axis is another pivotal component in gut-brain communication and allowing the gut to influence mood, such as anxiety [23] (Fig. 4A). We found that the numbers of Crh^{+} (corticotropin releasing hormone) and Avp^{+} (arginine vasopressin) cells were comparable in the paraventricular nucleus (PVN) between WT and ERβ$^{-/-}$ mice (Fig. 4B-I, N, O). While the numbers of Crh^{+} and Avp^{+} cells in the PVN were significantly increased in the ERβ$^{-/-}$ mice on day 5 post-DSS compared with DSS-treated WT mice (Fig. 4 B-I, N, O). Oxytocin (Oxt) also mediates the regulation of HPA axis activity [31]. DSS-treated ERβ$^{-/-}$ mice showed higher number of Oxt^{+} cells in the PVN than control ERβ$^{-/-}$ or DSS-treated WT mice on day 5 post-DSS (Fig. 4J-M, P).

It's reported that co-release of Crh and Avp potentiates the corticosterone and

adrenocorticotropic hormone (ACTH) release toward stressor [32]. Corticosterone and ACTH levels were assessed by enzyme linked immunosorbent assay. It showed that DSS-treated ERβ$^{-/-}$ mice presented elevated plasma corticosterone and ACTH compared to DSS-treated WT mice or control ERβ$^{-/-}$ mice 5 days after DSS exposure (Fig. 4Q, R). Overall, ERβ deletion elicited elevated HPA responsiveness following DSS treatment, indicating that HPA axis hyperactivity exerts critical role in anxiety-like behaviors observed in DSS-treated ERβ$^{-/-}$ mice.

ErbB4 was downregulated in the hypothalamus of ERβ$^{-/-}$ mice with experimental colitis.

To uncover potential molecular mechanisms underlying the increased anxiety-like behaviors in ERβ-deficiency mice with colitis, we performed RNA sequencing (RNA-seq) analysis of hypothalamus from WT and ERβ$^{-/-}$ mice on day 5. The gene expression profile in hypothalamus of WT control, ERβ$^{-/-}$ control, DSS treated WT, and DSS treated ERβ$^{-/-}$ mice were shown in hierarchical clustering heatmap (Fig. 5A). Higher expressions of several hypothalamic neuropeptides were found in ERβ$^{-/-}$ mice treated with DSS (Fig. S6), which further confirms the role of hypothalamus in anxiety disorder caused by ERβ$^{-/-}$ deficiency during colitis. Venn diagram showed there were1489 DSS regulated different expressed genes (DEGs) between control ERβ$^{-/-}$ mice and DSS-treated ERβ$^{-/-}$ mice, and 1325 ERβ regulated DEGs between DSS-treated ERβ$^{-/-}$ and DSS-treated WT, 934 genes that were co-regulated by DSS and ERβ among these DEGs (Fig. 5B). And hierarchical clustering analysis of the 934 co-regulated genes showed the ERβ deletion had the significant effects of DSS on the co-regulated genes (Fig. S7). It has been reported that ErbB4 is involved in regulating various neuropsychiatric disorders, including

schizophrenia [33], anxiety [34] and seizure [35], and this receptor is mostly expressed in PVN of hypothalamus [36]. In accordance, ErbB signaling pathway was found to significant enrichment in KEGG pathways (Fig. 5C, D). The gene expressions of *ErbB4* and its several downstream genes (*Pik3ca*, *Pik3r1*, *Akt2*, *Gsk3b* and *Cdkn1a*) in the hypothalamus were further identified by quantitative real-time PCR. Decreased mRNA levels of *ErbB4*, *Pik3ca*, *Pik3r1*, *Akt2*, *Gsk3b* and *Cdkn1a* were shown in DSS-treated ERβ$^{-/-}$ mice compared with DSS-treated WT mice (Fig. 5E). We next conducted the immunofluorescence staining to verify the protein expression level of ErbB4 in hypothalamus (Fig. 5F, G). The number of ErbB4^{+} cells in the hypothalamic PVN of ERβ$^{-/-}$ mice was comparable to that in WT mice (Fig. 5F, G). However, the ErbB4^{+} cell number in the PVN of DSS-treated ERβ$^{-/-}$ mice was significantly reduced compared with DSS-treated WT mice on day 5 post-DSS (Fig. 5F, G). Given decreased ErbB4 expression in hypothalamus of ERβ$^{-/-}$ mice in response to DSS as well as its established role in regulating brain functions, we hypothesized that ErbB4 may be an important regulator in anxiety-like behavior in ERβ$^{-/-}$ mice with colitis.

Gut microbiota of ERβ$^{-/-}$ mice was sufficient to facilitate DSS colitis and anxiety-like behaviors.

To probe if the DSS-induced colitis severity and anxiety-like behaviors in ERβ$^{-/-}$ mice correlate with the changes of gut microbiota, the microbiota transfer studies by co-housing of WT and ERβ$^{-/-}$ mice were performed, in which mice were exposed to the microbiota of each other based on their coprophagia (Fig. 6A). The PCoA plot revealed an equilibrated gut microbial landscape in CoHo mice before treated with DSS (Fig. 6B). We further assessed the co-housing procedure on the abundances of specific bacteria before treated

with DSS. The abundances of genus *Bacteroides* and *Prevotellaceae_UGC_001*, and family *Bacteroidaceae, Prevotellaceae* and *Veillonellaceae* were similar in CoHo WT and CoHo ERβ$^{-/-}$ mice (Fig. S8).

Then, the colitis severity, anxiety-like behaviors, levels of stress-related hormones and expression of ErbB4 were evaluated in SiHo WT mice, SiHo ERβ$^{-/-}$ mice, CoHo WT and CoHo ERβ$^{-/-}$ mice after treated with DSS. In line with our aforementioned results, SiHo ERβ$^{-/-}$ mice were susceptible to DSS-induced colitis (Fig. 6C, D) and related anxiety-like behaviors compared to SiHo WT mice (Fig. 6E-G). Of note, based on altered gut microbiota in CoHo mice, there were also significant difference in their clinical activity related colitis. Compared with SiHo WT mice, CoHo WT mice showed a tendency towards lower body weight (Fig. 6C), aggravated colitis severity (Fig. 6D), and more severe anxiety-like behaviors (less time and frequency into the center area of open field, more time in dark side of light-dark box) (Fig. 6E-G). Furthermore, plasma levels of corticosterone and ACTH showed upward tendencies in CoHo WT mice compared with SiHo WT mice (Fig. 6H, I). The immunofluorescence staining showed that the number of ErbB4 positive cells was reduced in the PVN of CoHo WT mice compared with SiHo WT mice after treated with DSS (Fig. 6J, K).

The above evidences suggested that gut microbiota dysbiosis contributed to the elevated colitis severity and related anxiety-like behaviors in ERβ$^{-/-}$ mice, and decreased hypothalamic ErbB4 expression might mediate the increased HPA axis activity and anxiety in ERβ-deficiency mice compared with WT mice when suffering from visceral stress from gut.

Discussion

In the present study, we provide evidence that ERβ deficiency resulted in multiple behavioral abnormalities indicative of anxiety, impaired the gut microbiota composition of mice, and increased susceptibility to DSS-induced colitis. We showed that highly coordinated differential gene expressions in the hypothalamus, a key brain region of anxiety and stress, which may contribute to the elicited anxiety like behavior of DSS-treated ERβ$^{-/-}$ mice. In addition, more severe colitis and anxiety-like behaviors were detected in the WT mice with DSS-induced colitis, when the gut microbial landscape was equilibrated by cohousing, unequivocally showing that gut microbiota is responsible for the deleterious effects on the gut and behavior of ERβ-deficiency mice with colitis.

IBD is a chronic and devastating gastrointestinal disease, and is usually complicated by psychological comorbidities. It has been reported that up to 60-80% IBD patients with active disease and 30% with clinical remission suffer from mood disorders, especially anxiety and depression [37]. Nowadays, clinicians raise an idea that exploring integrated model of care for both psychological and physiological disorders in IBD patients [38]. However, the connections between mental disorders and IBD are complex and still unclear. In the present study, we found that ERβ deficiency caused elevated anxiety-like behaviors in mice treated with DSS, while did not affect depression-like behaviors, sensorimotor functions, memory functions and social interaction. Our findings suggest that ERβ is a protective gene conferring resilience to anxiety when mice were suffering from colitis. The susceptibility to anxiety disorders has been also shown in other models when ERβ is deficient [39]. However, the underlying mechanisms are still not fully understood.

A growing body of evidence indicates that gut microbiota is involved in mental health

[40, 41]. We found that the fecal microbiota community richness (alpha diversity) and microbiota composition (beta diversity) were significantly changed either under baseline conditions or inflammatory state. The ERβ$^{-/-}$ mice under baseline conditions displayed significant alterations in gut microbiota composition, and concerned an enrichment of *Bacteroides*, *Prevotellaceae_UCG_001* and *Quinella* at genus level, and *Veillonellaceae* at family level. Furthermore, the abundance of *Prevotellaceae_UCG_001* was higher in DSS-treated ERβ$^{-/-}$ mice compared with DSS-treated WT mice. Chen and Jiang et al. [42, 43] found that the abundance of *Bacteroides* were positively associated with anxiety severity in patients with generalized anxiety disorder. Comorbid inflammatory bowel syndrome and anxiety/depression also had higher abundance of *Prevotella/Prevotellaceae* and *Bacteroides* [44]. *Bacteroides* and *Prevotellaceae_UCG_001* might be the key bacteria that regulate anxiety disorder in ERβ$^{-/-}$ mice with colitis.

The gut inflammatory responses act as important bridge link the gut microbiota and anxiety disorder [25, 26]. Jang et al. [45] found that dysbiosis caused by ampicillin could induce gastrointestinal inflammation, which further resulted in anxiety-like behaviors in mice. De Palma et al. [8] demonstrated that transplantation of fecal microbiota from inflammatory bowel syndrome patients altered the expression of inflammation-related genes in colonic tissues, and caused anxiety-like behaviors in the recipient mice. In the present study, ERβ$^{-/-}$ mice exposed to DSS exhibited apparent signs of colitis, more severe colonic ulceration, crypt damage and inflammation compared with DSS-treated WT mice. The dysbiosis induced by ERβ deficiency might contribute to elevated levels of colon inflammation. *Prevotellaceae*, *Bacteroidaceae* and *Veillonellaceae* families, which are reported to be involved in the pathogenesis of IBD by interacting with host genetics.

Gpr109a$^{-/-}$Rag1$^{-/-}$ mice showed spontaneous rectal prolapse and colonic inflammation, whose gut was colonized increased abundances of *Bacteroidaceae* and *Prevotellaceae* [46]. NHE3$^{-/-}$ was characterized by an expansion of *Bacteroidaceae*, and the onset and severity of experimental colitis were aggravated in the recipient mice received the microbiota of NHE3$^{-/-}$ mice [47]. Members of *Veillonellaceae* are associated with many chronic inflammatory diseases, including IBD, and its abundance was increased in Nlrx1$^{-/-}$ mice or in WT mice cohoused with Nlrx1$^{-/-}$ mice which caused worse DSS-induced colitis [48].

Previous studies have indicated that the inflammatory responses and HPA axis hyperactivity seem to be plausible mechanisms developed to explain behavior alterations induced by gut dysbiosis[28, 45, 49]. Amygdala, hypothalamus, mPFC, and ventral hippocampus are vital brain regions related to anxiety disorder. Here, we found that there was no significant difference in neuroinflammation of mPFC, amygdala and ventral hippocampus between DSS-treated WT mice and DSS-treated ERβ$^{-/-}$ mice in the aspect of microglia cells density. It is well known that stress, including visceral stress and systemic pro-inflammatory cytokines, activates the secretion of the Crh from hypothalamus, stimulates ACTH secretion from the pituitary gland, which leads to the release of corticosterone, and causes anxiety disorder [37]. We observed that the corticosterone and ACTH levels in the plasma were elevated in ERβ$^{-/-}$ mice after treatment with DSS. The hypothalamus is considered the starting point of the HPA axis, the number of Crh^{+}, Avp^{+} and Oxt^{+} cells in the PVN were also increased in the ERβ$^{-/-}$ mice followed by DSS treatment. Our data suggests that changes in HPA axis rather than neuroinflammation is the underlying mechanism how dysbiosis caused by ERβ deficiency influenced anxiety-like behaviors.

The transcriptome data point to the ErbB pathway, especially ErbB4 pathway, is

downregulated in the hypothalamus of ERβ$^{-/-}$ mice following DSS treatment compared with DSS-treated WT mice. Moreover, both the mRNA expression of ErbB4 in the hypothalamus and number of ErbB4^{+} cells in the PVN were reduced significantly in the DSS-treated ERβ$^{-/-}$ mice. It has been confirmed that ErbB4 is highly expressed in the hypothalamus, especially in PVN [36]. Remarkably, alterations of ErbB4 expression in amygdala [50, 51] and white matter [52] could exert anxiety-like behaviors in mice. It is important to note that activated Nrg1/ErbB4 signaling could partly normalized the stress-induced behavioral changes in rats [53]. These evidences provide hypotheses that ErbB4 might be an important regulator of HPA axis activation and progression of anxiety disorder in ERβ-deficiency mice treated with DSS.

Numerous studies have indicated that colitis and anxiety-like behaviors could be profoundly influenced by transmissible microbial compositions arised from diet changes or host genetic defects [54-56]. After we transferred ERβ$^{-/-}$ mice fecal microbiota to WT mice by co-housing, the gut microbiota composition of CoHo WT mice displayed almost comparable to the one of ERβ$^{-/-}$ mice. There is a growing body of evidence for the shifts in gut microbiota composition influencing anxiety-like behaviors through the microbiota-gut-brain axis [57]. In agreement with these findings, we report herein that colonization of WT mice with gut microbiota from ERβ$^{-/-}$ mice using co-housing, is sufficient to drive anxiety-like behaviors in mice following DSS treatment. Moreover, the CoHo WT mice exhibited a more severe colitis severity compared with SiHo WT mice. These results establish the harmful nature of ERβ-deficiency shifted gut microbiota composition, and ERβ might exert protective effects for microbial symbiosis, reduce the colitis susceptibility and related anxiety-like behavior. In comparison with DSS-treated SiHo WT mice, DSS-treated CoHo

WT mice showed a trend to increased corticosterone levels in the plasma and lower expression of ErbB4 in hypothalamus, indicating gut microbiota alteration might be involved in the HPA axis hyperactivity and elicited anxiety-like behaviors through regulating ErbB4 expression in the hypothalamus.

In summary, we have shown that gut dysbiosis induced by ERβ deficiency is crucial in the development of IBD and related anxiety-like behavior by regulating HPA axis hyperactivity. Downregulation of ErbB4 in the hypothalamus is a potential mechanism in the modulating HPA axis hyperactivity. Our findings highlight the novel role of ERβ in gut-brain communications, and provides a possible therapeutic approach for the treatment of psychiatric co-morbidities in IBD.

List of abbreviations

AB-PAS, alcian-blue periodic acid schiff; ACTH, adrenocorticotropic hormone; Avp, arginine vasopressin; CNS, central nervous system; CoHo, co-housed; Crh, corticotropin releasing hormone; DSS, dextran sodium sulphate; Elisa, enzyme linked immunosorbent assay; ER, estrogen receptor; HE, hematoxylin and eosin; HPA, hypothalamic-pituitary-adrenal; IBD, inflammatory bowel disease; Oxt, oxytocin; PCoA, principal component analysis; PVN, paraventricular nucleus; RNA-seq, RNA sequencing; SiHo, single-housed.

Declarations

Ethics approval and consent to participate

The experimental procedures were carried out in line with the Guidelines for Animal Committee of Third Military Medical University.

Consent for publication

Not applicable.

Availability of data and materials

All data generated or analysed during this study are included in this published article and its supplementary information files, and deposited at the NCBI Sequence Read Archive (SRA) under the accession number PRJNA632986.

Competing interests

The authors declare that they have no competing interests.

Funding

This work was supported by the National Key R&D Program of China (2017YFE0103700), and National Nature Science Foundation of China (No. 31871043).

Authors' contributions

Conceptualization: XF, JAG, XX, YM; Experimentation: YM, TL, XL, AK, RX, RX, JG, ZW, YC, LY; Data analysis: YM, TL, XL, LW, JZ, JZ; Manuscript preparation and revision: XF, JAG, HX, XX, YM, TL, MW. All authors contributed to the final version of the manuscript.

Acknowledgements

This work was supported by the National Key R&D Program of China (2017YFE0103700), and National Nature Science Foundation of China (No. 31871043). We thank L. Wei (State Key Laboratory of Ophthalmology, Zhongshan Ophthalmic Center, Sun Yat-sen University) for valuable suggestions about the manuscript.

References

1. Caruso R, Lo BC, Nunez G. Host-microbiota interactions in inflammatory bowel disease. Nat Rev Immunol. 2020; 9(379).
2. Regueiro M, Greer JB, Szigethy E. Etiology and treatment of pain and psychosocial issues in patients with inflammatory bowel diseases. Gastroenterology. 2017; 152(2):430-9.e434.
3. Barberio B, Zamani M, Black CJ, Savarino EV, Ford AC. Prevalence of symptoms of anxiety and depression in patients with inflammatory bowel disease: a systematic review and meta-analysis. Lancet Gastroenterol Hepatol. 2021; 6(5):359-70.
4. Gracie DJ, Williams CJ, Sood R, Mumtaz S, Bholah MH, Hamlin PJ *et al*. Poor correlation between clinical disease activity and mucosal inflammation, and the role of psychological comorbidity, in inflammatory bowel disease. Am J Gastroenterol. 2016; 111(4):541-51.
5. Ni J, Wu GD, Albenberg L, Tomov VT. Gut microbiota and IBD: causation or correlation? Nat Rev Gastroenterol Hepatol. 2017; 14(10):573-84.
6. Franzosa EA, Sirota-Madi A, Avila-Pacheco J, Fornelos N, Haiser HJ, Reinker S *et al*. Gut microbiome structure and metabolic activity in inflammatory bowel disease. Nat Microbiol. 2019; 4(2):293-305.
7. Britton GJ, Contijoch EJ, Mogno I, Vennaro OH, Llewellyn SR, Ng R *et al*. Microbiotas from humans with inflammatory bowel disease alter the balance of gut Th17 and RORgammat(+) regulatory T cells and exacerbate colitis in mice. Immunity. 2019; 50(1):212-24 e214.
8. De Palma G, Lynch MD, Lu J, Dang VT, Deng Y, Jury J *et al*. Transplantation of fecal microbiota from patients with irritable bowel syndrome alters gut function

and behavior in recipient mice. Sci Transl Med. 2017; 9(379).

9. Kilinçarslan S, Evrensel A. The effect of fecal microbiota transplantation on psychiatric symptoms among patients with inflammatory bowel disease: an experimental study. Actas espanolas de psiquiatria. 2020; 48(1):1-7.

10. Sanders ME, Merenstein DJ, Reid G, Gibson GR, Rastall RA. Probiotics and prebiotics in intestinal health and disease: from biology to the clinic. Nat Rev Gastroenterol Hepatol. 2019; 16(10):605-16.

11. Barbosa RSD, Vieira-Coelho MA. Probiotics and prebiotics: focus on psychiatric disorders - a systematic review. Nutr Rev. 2019; 78(6):437-50.

12. de Souza HSP, Fiocchi C, Iliopoulos D. The IBD interactome: an integrated view of aetiology, pathogenesis and therapy. Nat Rev Gastroenterol Hepatol. 2017; 14(12):739-49.

13. Chu H, Khosravi A, Kusumawardhani IP, Kwon AH, Vasconcelos AC, Cunha LD *et al*. Gene-microbiota interactions contribute to the pathogenesis of inflammatory bowel disease. Science (New York, NY). 2016; 352(6289):1116-20.

14. Wada-Hiraike O, Imamov O, Hiraike H, Hultenby K, Schwend T, Omoto Y *et al*. Role of estrogen receptor β in colonic epithelium. Proc Natl Acad Sci U S A. 2006; 103(8):2959-64.

15. Looijer-van Langen M, Hotte N, Dieleman LA, Albert E, Mulder C, Madsen KL. Estrogen receptor-beta signaling modulates epithelial barrier function. Am J Physiol Gastrointest Liver Physiol. 2011; 300(4):G621-6.

16. Warner M, Huang B, Gustafsson JA. Estrogen receptor beta as a pharmaceutical target. Trends Pharmacol Sci. 2017; 38(1):92-9.

17. Shin J-H, Park Y-H, Sim M, Kim S-A, Joung H, Shin D-M. Serum level of sex steroid hormone is associated with diversity and profiles of human gut microbiome. Res Microbiol. 2019; 170(4):192-201.

18. Ibrahim A, Hugerth L, Hases L, Saxena A, Seifert M, Thomas Q *et al*. Colitis-induced colorectal cancer and intestinal epithelial estrogen receptor beta impact gut microbiota diversity. Int J Cancer. 2018; 144(2):3086-98.

19. Lund TD, Rovis T, Chung WC, Handa RJ. Novel actions of estrogen receptor-beta on anxiety-related behaviors. Endocrinology. 2005; 146(2):797-807.

20. Krege JH, Hodgin JB, Couse JF, Enmark E, Warner M, Mahler JF *et al*. Generation and reproductive phenotypes of mice lacking estrogen receptor β. Proc Natl Acad Sci U S A. 1998; 95(26):15677-82.

21. Darnaud M, Santos AD, Gonzalez P, Augui S, Lacoste C, Desterke C *et al*. Enteric delivery of regenerating family member 3 alpha alters the intestinal microbiota and controls inflammation in mice with colitis. Gastroenterology. 2017; 154:1009-23.

22. Gracie DJ, Guthrie EA, Hamlin PJ, Ford AC. Bi-directionality of brain-gut interactions in patients with inflammatory bowel diseases. Gastroenterology. 2018; 154(6):1635-46. e3.

23. Huo R, Zeng B, Zeng L, Cheng K, Li B, Luo Y *et al*. Microbiota modulate anxiety-like behavior and endocrine abnormalities in hypothalamic-pituitary-adrenal axis. Front Cell Infect Microbiol. 2017; 7:489.

24. Pan JX, Deng FL, Zeng BH, Zheng P, Liang WW, Yin BM *et al*. Absence of gut microbiota during early life affects anxiolytic behaviors and monoamine neurotransmitters system in the hippocampal of mice. J Neurol Sci. 2019; 400:160-

8.

25. El Aidy S, Dinan TG, Cryan JF. Immune modulation of the brain-gut-microbe axis. Front Microbiol. 2014; 5:146.

26. Lee Y, Kim YK. Understanding the connection between the gut-brain axis and stress/anxiety disorders. Curr Psychiatry Rep. 2021; 23(5):22.

27. Jang SE, Lim SM, Jeong JJ, Jang HM, Lee HJ, Han MJ *et al*. Gastrointestinal inflammation by gut microbiota disturbance induces memory impairment in mice. Mucosal Immunol. 2017; 11(2):369-79.

28. Dempsey E, Abautret-Daly Á, Docherty NG, Medina C, Harkin A. Persistent central inflammation and region specific cellular activation accompany depression- and anxiety-like behaviours during the resolution phase of experimental colitis. Brain Behav Immun. 2019; 80:616-32.

29. Yagihashi M, Kano M, Muratsubaki T, Morishita J, Kono K, Tanaka Y *et al*. Concordant pattern of the HPA axis response to visceral stimulation and CRH administration. Neurosci Res. 2021; 168:32-40.

30. Rackers HS, Thomas S, Williamson K, Posey R, Kimmel MC. Emerging literature in the microbiota-brain axis and perinatal mood and anxiety disorders. Psychoneuroendocrinology. 2018; 95:86-96.

31. Jurek B, Neumann ID. The oxytocin receptor: from intracellular signaling to behavior. Physiol Rev. 2018; 98(3):1805-908.

32. Keller-Wood M. Hypothalamic-Pituitary-Adrenal Axis—Feedback Control. In: Compr Physiol. 2015; 1161-82.

33. Pitcher GM, Kalia LV, Ng D, Goodfellow NM, Yee KT, Lambe EK *et al*.

Schizophrenia susceptibility pathway neuregulin 1-ErbB4 suppresses Src upregulation of NMDA receptors. Nat Med. 2011; 17(4):470-8.

34. Bi LL, Sun XD, Zhang J, Lu YS, Chen YH, Wang J *et al*. Amygdala NRG1-ErbB4 is critical for the modulation of anxiety-like behaviors. Neuropsychopharmacology. 2015; 40(4):974-86.

35. Tan GH, Liu YY, Hu XL, Yin DM, Mei L, Xiong ZQ. Neuregulin 1 represses limbic epileptogenesis through ErbB4 in parvalbumin-expressing interneurons. Nat Neurosci. 2011; 15(2):258-66.

36. Bean JC, Lin TW, Sathyamurthy A, Liu F, Yin DM, Xiong WC *et al*. Genetic labeling reveals novel cellular targets of schizophrenia susceptibility gene: distribution of GABA and non-GABA ErbB4-positive cells in adult mouse brain. J Neurosci. 2014; 34(40):13549-66.

37. Ancona A, Petito C, Iavarone I, Petito V, Galasso L, Leonetti A *et al*. The gut-brain axis in irritable bowel syndrome and inflammatory bowel disease. Dig Liver Dis. 2021; 53(3):298-305.

38. Fairbrass KM, Gracie DJ. Mood and treatment persistence in inflammatory bowel disease: time to consider integrated models of care? Clin Gastroenterol Hepatol. 2021; 19(6):1111-13.

39. Borrow AP, Handa RJ. Estrogen receptors modulation of anxiety-like behavior. Vitam Horm. 2017; 103:27-52.

40. Fond GB, Lagier J-C, Honore S, Lancon C, Korchia T, Sunhary De Verville P-L *et al*. Microbiota-orientated treatments for major depression and schizophrenia. Nutrients. 2020; 12(4):1024.

41. Järbrink-Sehgal E, Andreasson A. The gut microbiota and mental health in adults. Curr Opin Neurobiol. 2020; 62:102-14.

42. Chen YH, Bai J, Wu D, Yu SF, Qiang XL, Bai H *et al*. Association between fecal microbiota and generalized anxiety disorder: severity and early treatment response. J Affect Disord. 2019; 259:56-66.

43. Jiang HY, Zhang X, Yu ZH, Zhang Z, Deng M, Zhao JH *et al*. Altered gut microbiota profile in patients with generalized anxiety disorder. J Psychiatr Res. 2018; 104:130-36.

44. Simpson CA, Mu A, Haslam N, Schwartz OS, Simmons JG. Feeling down? A systematic review of the gut microbiota in anxiety/depression and irritable bowel syndrome. J Affect Disord. 2020; 266:429-46.

45. Jang HM, Lee HJ, Jang SE, Han MJ, Kim DH. Evidence for interplay among antibacterial-induced gut microbiota disturbance, neuro-inflammation, and anxiety in mice. Mucosal Immunol. 2018; 11(5): 1386-97.

46. Bhatt B, Zeng P, Zhu H, Sivaprakasam S, Li S, Xiao H *et al*. Gpr109a limits microbiota-induced IL-23 production to constrain ILC3-mediated colonic inflammation. J Immunol. 2018; 200(8):2905-14.

47. Harrison CA, Laubitz D, Ohland CL, Midura-Kiela MT, Patil K, Besselsen DG *et al*. Microbial dysbiosis associated with impaired intestinal Na(+)/H(+) exchange accelerates and exacerbates colitis in ex-germ free mice. Mucosal Immunol. 2018; 11(5):1329-41.

48. Leber A, Hontecillas R, Tubau-Juni N, Zoccoli-Rodriguez V, Abedi V, Bassaganya-Riera J. NLRX1 modulates immunometabolic mechanisms controlling the host-gut

microbiota interactions during inflammatory bowel disease. Front Immunol. 2018; 9:363.

49. Foster JA, McVey Neufeld KA. Gut-brain axis: how the microbiome influences anxiety and depression. Trends Neurosci. 2013; 36(5):305-12.

50. Ahrens S, Wu MV, Furlan A, Hwang GR, Paik R, Li H *et al*. A central extended amygdala circuit that modulates anxiety. J Neurosci. 2018; 38(24):5567-83.

51. Geng F, Zhang J, Wu JL, Zou WJ, Liang ZP, Bi LL *et al*. Neuregulin 1-ErbB4 signaling in the bed nucleus of the stria terminalis regulates anxiety-like behavior. Neuroscience. 2016; 329:182-92.

52. Roy K, Murtie JC, El-Khodor BF, Edgar N, Sardi SP, Hooks BM *et al*. Loss of erbB signaling in oligodendrocytes alters myelin and dopaminergic function, a potential mechanism for neuropsychiatric disorders. Proc Natl Acad Sci U S A. 2007; 104(19):8131-36.

53. Dang R, Cai H, Zhang L, Liang D, Lv C, Guo Y *et al*. Dysregulation of Neuregulin-1/ErbB signaling in the prefrontal cortex and hippocampus of rats exposed to chronic unpredictable mild stress. Physiol Behav. 2016; 154:145-150.

54. Iyer SS, Gensollen T, Gandhi A, Oh SF, Neves JF, Collin F *et al*. Dietary and microbial oxazoles induce intestinal inflammation by modulating aryl hydrocarbon receptor responses. Cell. 2018; 173(5):1123-1134.e1111.

55. Darnaud M, Santos AD, Gonzalez P, Augui S, Lacoste C, Desterke C *et al*. Enteric delivery of regenerating family member 3 alpha alters the intestinal microbiota and controls inflammation in mice with colitis. Gastroenterology. 2017; 154(4):1009-23 e14.

56. Chinna Meyyappan A, Forth E, Wallace CJK, Milev R. Effect of fecal microbiota transplant on symptoms of psychiatric disorders: a systematic review. BMC psychiatry. 2020; 20(1):299.

57. Murray E, Sharma R, Smith KB, Mar KD, Barve R, Lukasik M *et al*. Probiotic consumption during puberty mitigates LPS-induced immune responses and protects against stress-induced depression- and anxiety-like behaviors in adulthood in a sex-specific manner. Brain Behav Immun. 2019; 81:198-212.

Figures

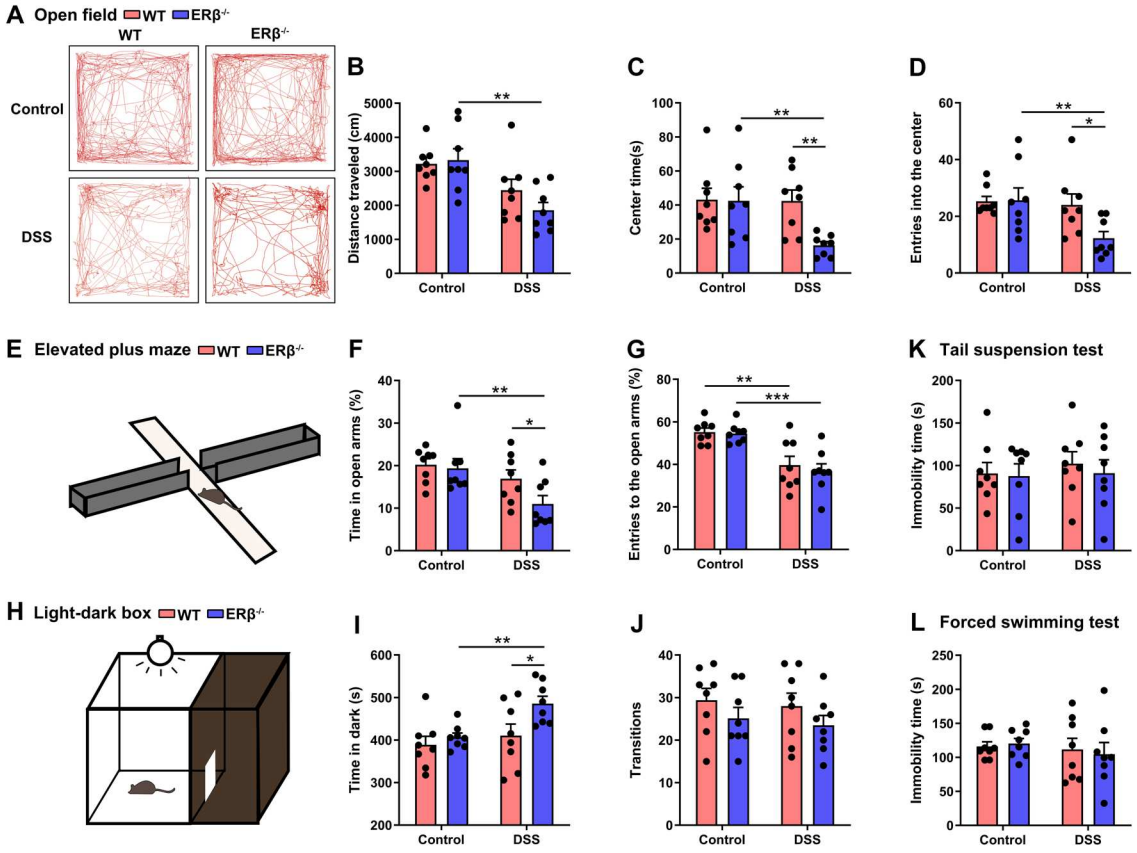

Figure 1. Increased anxiety-like behaviors in ERβ$^{-/-}$ mice following induced experimental colitis, but no significant depressive behaviors.

(A-D) Representative trajectory diagrams of 4 groups of mice in the open field test (A), and total distance traveled (B), time spent in the central zone (C) and entries into the center (D) of WT and ERβ$^{-/-}$ mice treated with water or DSS. **(E-G)** Diagram of elevated plus maze (E), and percentage of time mice spent in the open arms (F) and frequency of entries into the open arms (G) in the elevated-plus maze test. **(H-J)** Diagram of light-dark box (H), and time that mice spent in the dark chamber (I) and transitions between 2 chambers (J) in the light-dark box test. **(K, L)** The immobility time of mice among 4 groups in the tail suspension test (K) and forced swimming test (L). Data are presented as mean ± SEM.

Statistical comparison was performed by two-way ANOVA. n= 8/group. *P<0.05, **P<0.01, ***P<0.001.

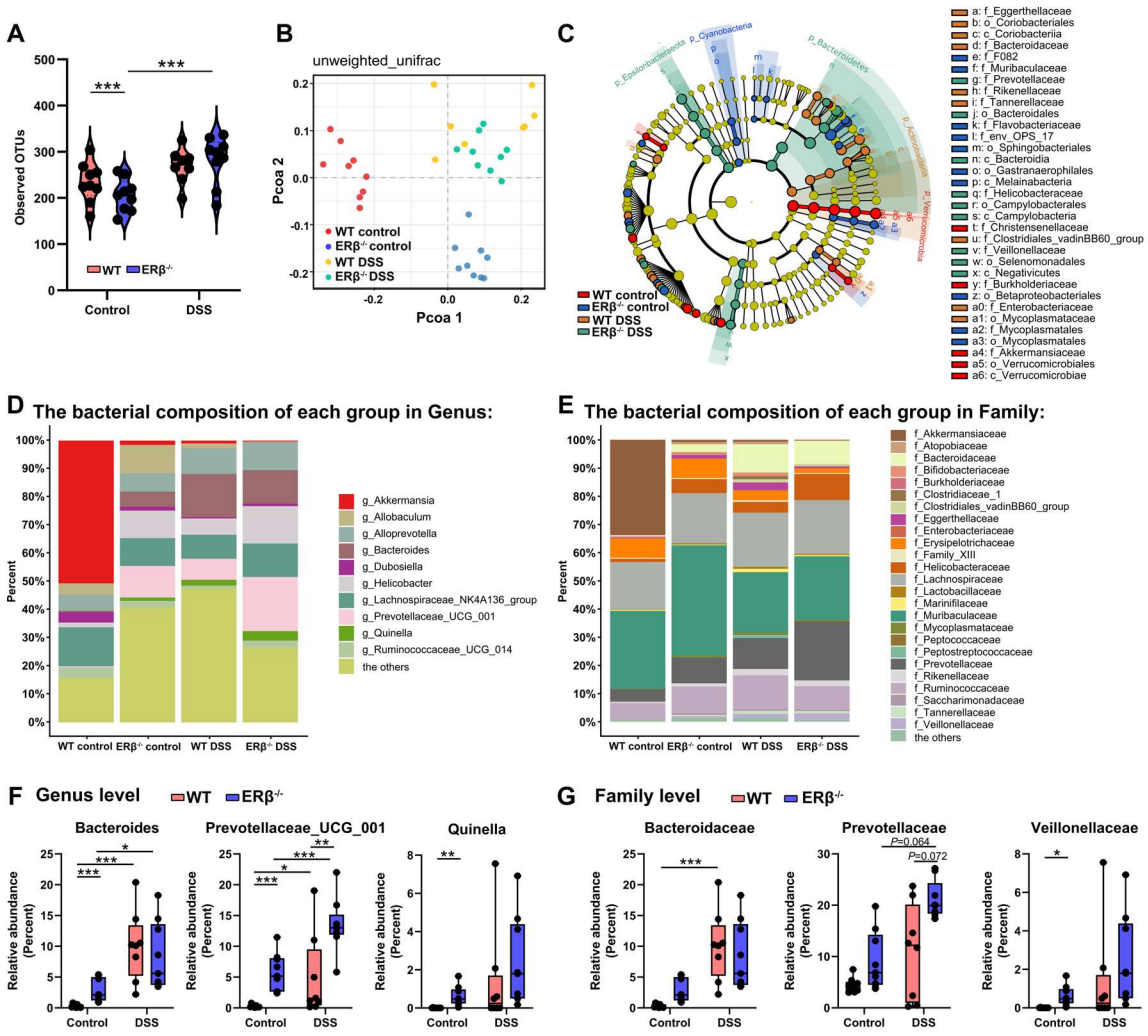

Figure 2. Differences in the fecal microbiota of WT and ERβ$^{-/-}$ mice under basal and inflammatory states.

(A) Community richness calculated by observed OTUs. **(B)** Principal coordinates analysis of microbial unweighted UniFrac compositional differences. **(C)** Taxonomic cladogram obtained using LEfSe analysis. **(D, E)** Bar graph of bacterial abundance in genus (D) and family (E) levels. **(F, G)** Relative abundances of substantially changed bacteria taxa in genus (F) and family (G) levels. Data are presented as boxplots. Statistical comparison was performed by non-parametric Wilcoxon rank sum. n=9/group, except for n=8 in WT DSS group. *P<0.05, **P<0.01, ***P<0.001.

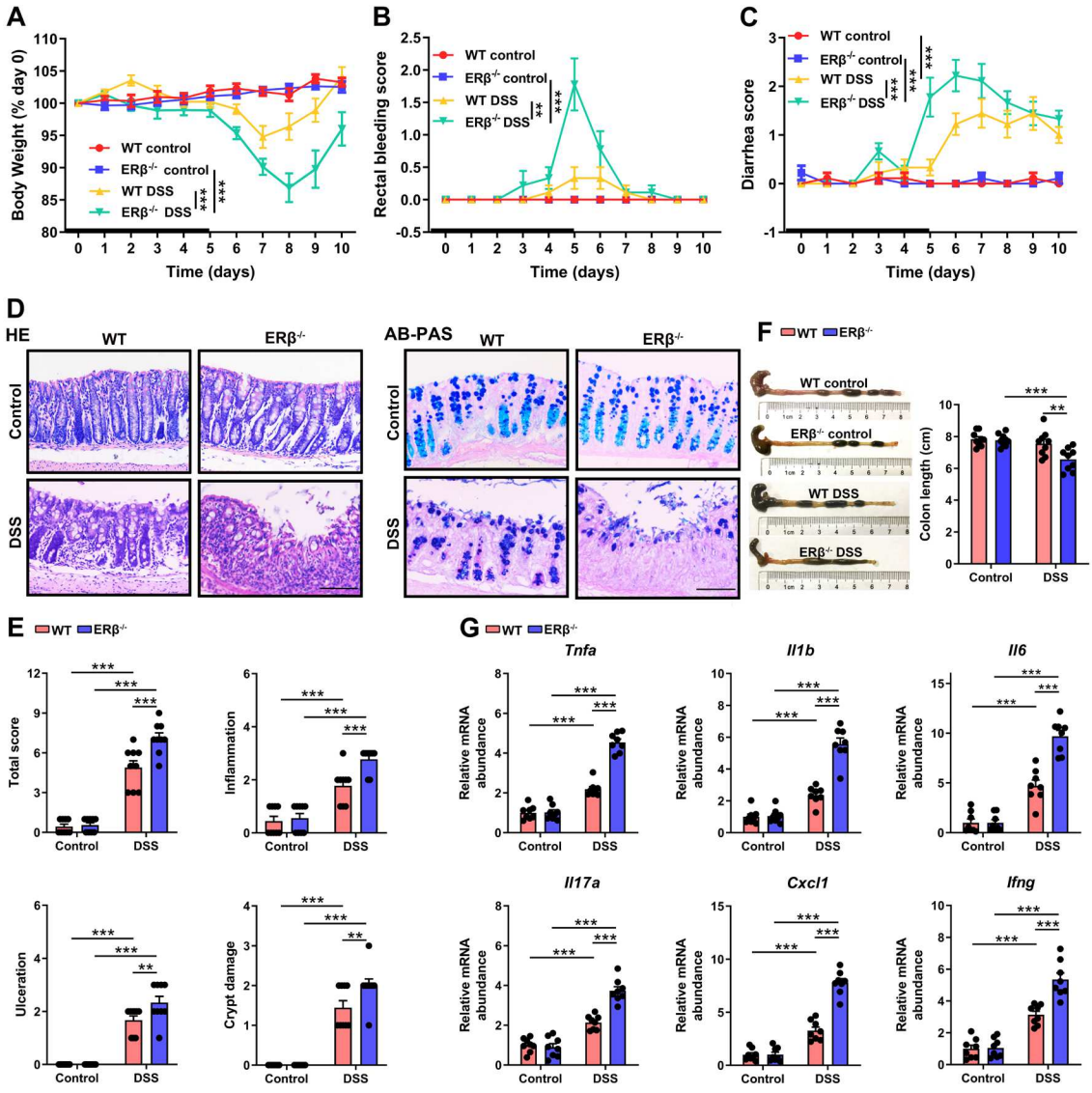

Figure 3. ERβ-deficiency aggravated the development of DSS-induced colitis.

(A-C) Time evolution of DSS-induced colitis in WT. Heavy line: 5-day period of DSS administration. Body weight (A), rectal bleeding score (B) and diarrhea score (C) were evaluated. n=9/group. **(D)** Histology of distal colon tissues collected at day 5 was examined by HE and AB-PAS. Scale bar=100 μm. **(E)** Composite score of histopathology (inflammation, ulceration and crypt damage scores). n=9/group. **(F)** Mice were killed on day 5 after DSS treatment to measure colon length. n=9/group. **(G)** Quantitative real-time

PCR analysis of mRNA expressions of inflammatory cytokines (*Tnfa*, *Il1b*, *Il6*, *Il17a*, *Cxcl1* and *Ifng*) in whole colon tissues. n=8/group. Data represent mean ± SEM. Statistical comparison was performed by two-way ANOVA. **P*<0.05, ***P*<0.01, ****P*<0.001.

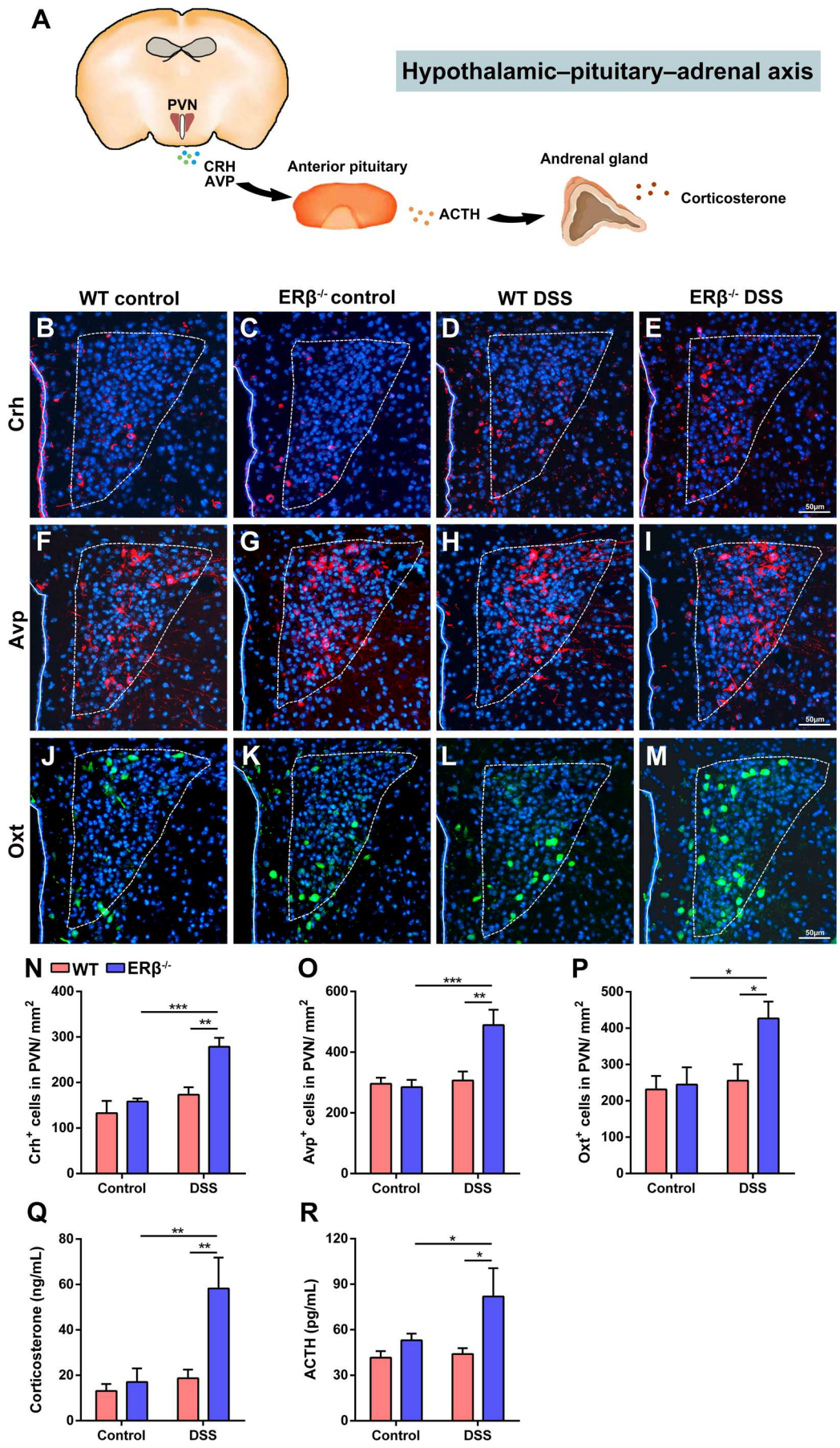
A
Hypothalamic–pituitary–adrenal axis
PVN
CRH
AVP
Anterior pituitary
ACTH
Andrenal gland
Corticosterone
WT control
ERβ-/- control
WT DSS
ERβ-/- DSS
Crh
Avp
Oxt
B
C
D
E
F
G
H
I
J
K
L
M
50μm
N
WT
ERβ-/-
Crh+ cells in PVN/ mm2
O
Avp+ cells in PVN/ mm2
P
Oxt+ cells in PVN/ mm2
Control
DSS
Q
Corticosterone (ng/mL)
R
ACTH (pg/mL)

Figure 4. Dysregulated hypothalamic-pituitary-adrenal axis in ERβ$^{-/-}$ mice with DSS-induced colitis.

(A) Diagram of hypothalamic-pituitary-adrenal axis. **(B-P)** Representative images and quantitative analysis of Crh (B-E, N), Avp (F-I, O) and Oxt (J-M, P) immunofluorescence staining within the PVN of WT and ERβ$^{-/-}$ mice under homeostatic and day 5 following DSS treatment. Scale bar=50 μm. n=5/group. **(Q, R)** Plasma corticosterone (Q) and ACTH (R) levels in basal conditions and 5 days after DSS treatment in WT and ERβ$^{-/-}$ mice. n=8/group. Data are presented as mean ± SEM. Statistical comparison was performed by two-way ANOVA. **P*<0.05, ***P*<0.01, ****P*<0.001.

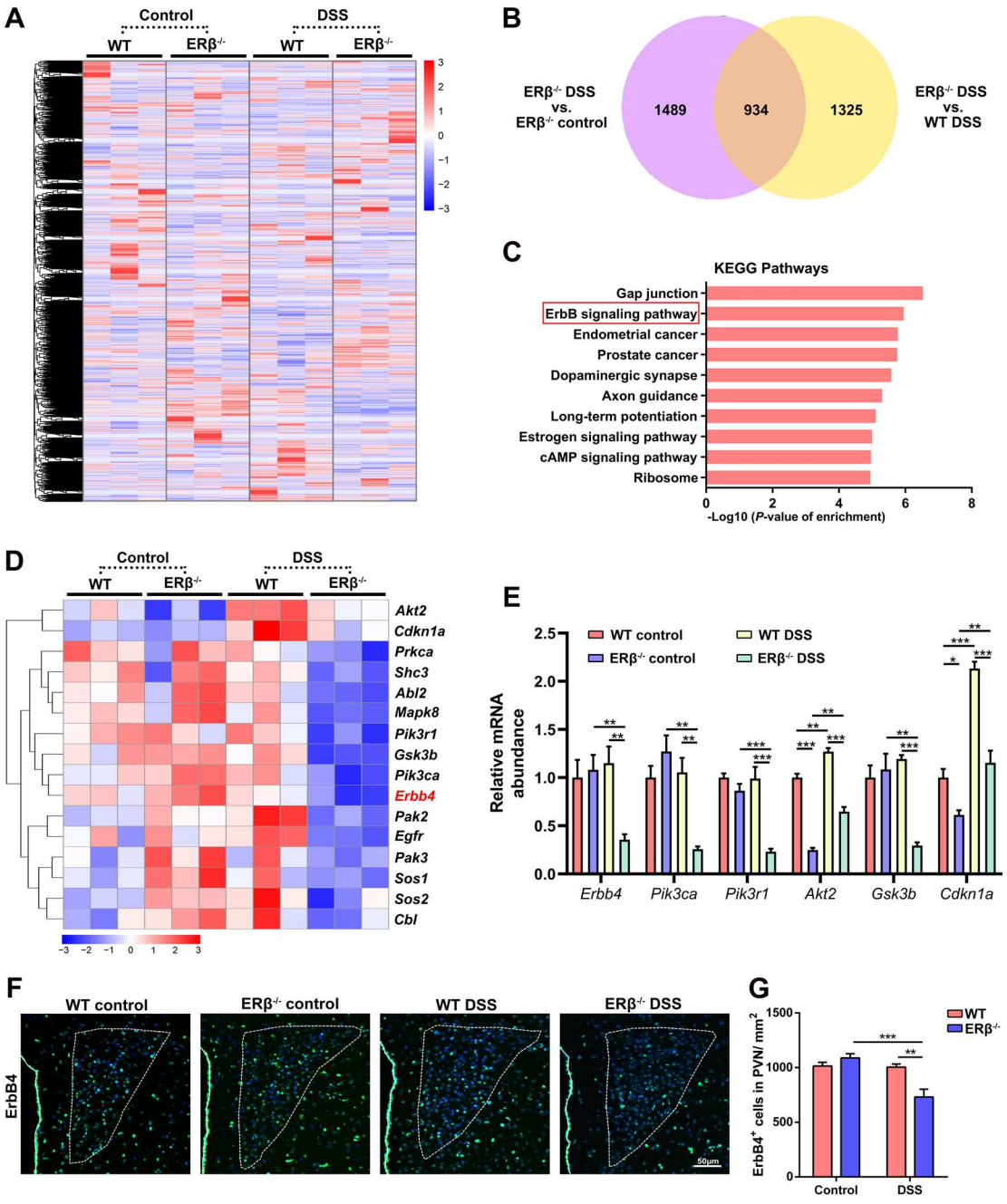

Figure 5. ErbB4 is downregulated in ERβ$^{-/-}$ mice with experimental colitis.

(A) Hierarchical clustering heatmap of gene expression profile in hypothalamus of WT and ERβ$^{-/-}$ mice under homeostasis status and treated with DSS. n=3/group. **(B)** Venn diagram of different expressed genes (DEGs) between control ERβ$^{-/-}$ and DSS ERβ$^{-/-}$ mice, and

DEGs between DSS ERβ$^{-/-}$ and DSS WT mice. n=3/group. **(C)** Signaling pathway enrichment analysis was performed using Kyoto Encyclopedia of Genes and Genomes (KEGG). Top 10 significantly enriched pathways in the hypothalamus of the overlapping 934 genes plotted by enrichment score. **(D)** Hierarchical clustering heatmap of gene expression profile of ErbB signaling pathway. n=3/group. **(E)** Quantitative real-time PCR analysis of mRNA expressions of *ErbB4* and its several downstream genes (*Pik3ca*, *Pik3r1*, *Akt2*, *Gsk3b* and *Cdkn1a*) in hypothalamus. n=3/group. **(F, G)** Representative images (F) and quantitative analysis (G) of ErbB4 immunofluorescence staining within the PVN of WT and ERβ$^{-/-}$ mice in the basal state and on day 5 after onset of exposure to DSS. Scale bar=50 μm. n=5/group. Data are presented as mean ± SEM. Statistical comparison was performed by two-way ANOVA. **P*<0.05, ***P*<0.01, ****P*<0.001.

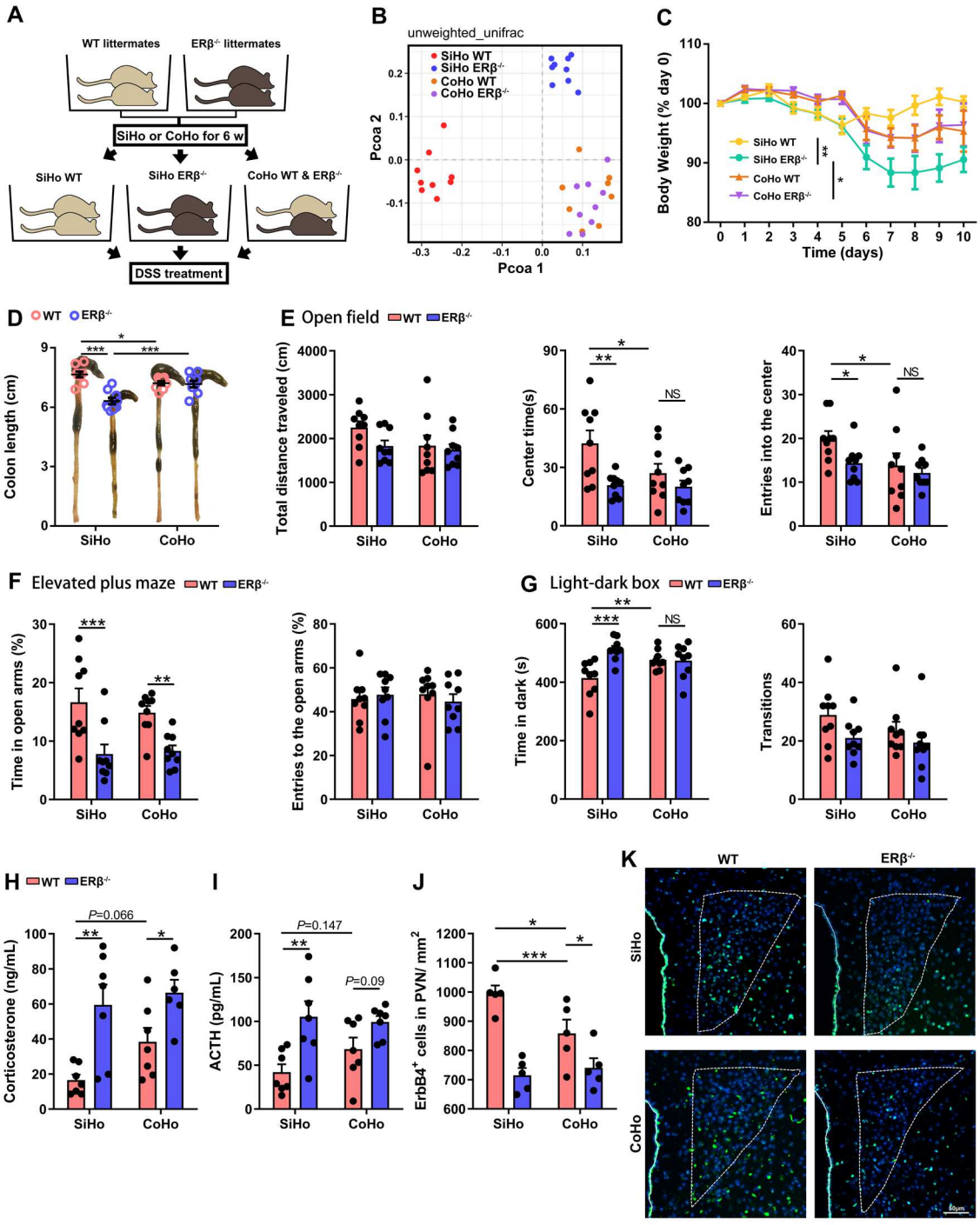

Figure 6. WT mice co-housed with ERβ$^{-/-}$ mice display aggravated colitis and increased anxiety-like behavior.

(A) Schematic representation of the cohousing and DSS treatment of WT and ERβ$^{-/-}$ mice.

(B) Principal coordinates analysis of microbial unweighted UniFrac compositional

differences among single-housed (SiHo) and co-housed (CoHo) WT and ERβ$^{-/-}$ mice before DSS treatment. n=9/group, except for n=8 in CoHo WT group. **(C)** Body weight of SiHo and CoHo WT and ERβ$^{-/-}$ mice at various times after treatment with DSS. n=9/group. **(D)** Colon length of SiHo and CoHo WT and ERβ$^{-/-}$ mice on day 5 following DSS treatment. n=9/group. **(E)** Total distance traveled, time spent in center, and entries into the center in the open-field test of SiHo and CoHo WT and ERβ$^{-/-}$ mice after DSS treatment. n=9/group. **(F)** Percentage of time spent in the open arms and percentage of the entries into the open arms in the elevated-plus maze test of DSS-treated SiHo and CoHo WT and ERβ$^{-/-}$ mice. n=9/group. **(G)** Time in dark and total transitions in the light-dark box test of DSS-treated SiHo and CoHo WT and ERβ$^{-/-}$ mice. n=9/group. **(H)** Plasma corticosteronelevels in SiHo and CoHo WT and ERβ$^{-/-}$ mice 5 days after DSS treatment. n=7/group, except for n=6 in CoHo ERβ$^{-/-}$ group. **(I)** Plasma ACTH levels in SiHo and CoHo WT and ERβ$^{-/-}$ mice 5 days post-DSS treatment. n=7/group. **(J, K)** Quantitative analysis (J) and representative images (K) of ErbB4 immunofluorescence staining within the PVN of SiHo and CoHo WT and ERβ$^{-/-}$ mice on day 5 after onset of exposure to DSS. Scale bar=50 μm. n=5/group. Data are presented as mean ± SEM. Statistical comparison was performed by two-way ANOVA. *P<0.05, **P<0.01, ***P<0.001.

Supplemental figures

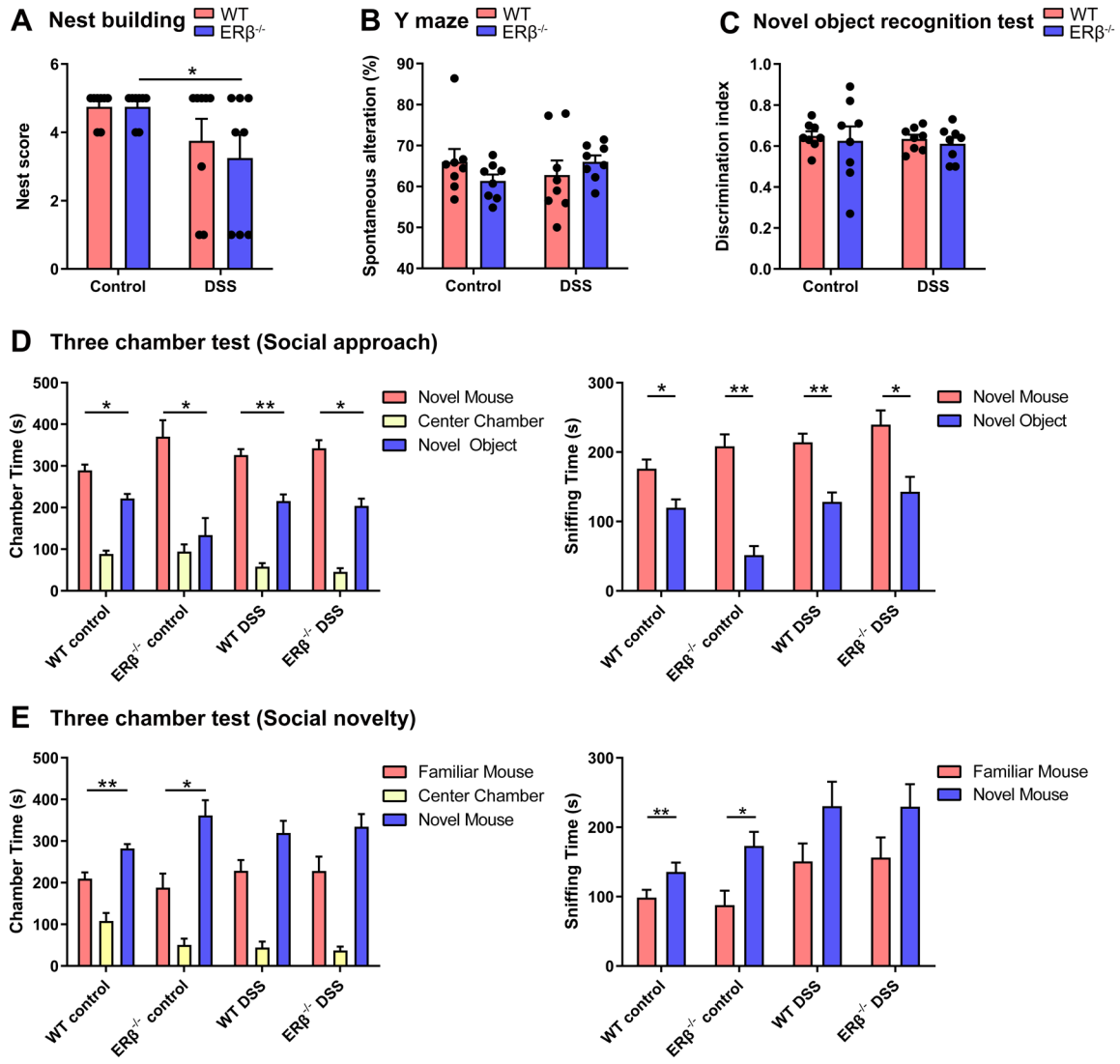

Figure S1. ERβ-deficiency did not influence the sensorimotor function, memory function and social interactions in mice following induced experimental colitis.

(A) Nest score in the nest building test among 4 groups was performed to detect sensorimotor functions. **(B)** Spatial memory was assessed by percentage spontaneous alteration in the Y maze test. **(C)** Recognition memory was detected by discrimination index in the novel object recognition test. **(D, E)** Time spent in each chamber and time sniffing novel mouse or novel object were used to test sociability in social approach period

(D). Social recognition was evaluated by time spent in each chamber and time sniffing familiar mouse or novel mouse in social novelty period (E). Data are presented as mean ± SEM. Statistical comparison was performed by two-way ANOVA, or paired t test for three chamber test. n= 8/group. *P<0.05, **P<0.01.

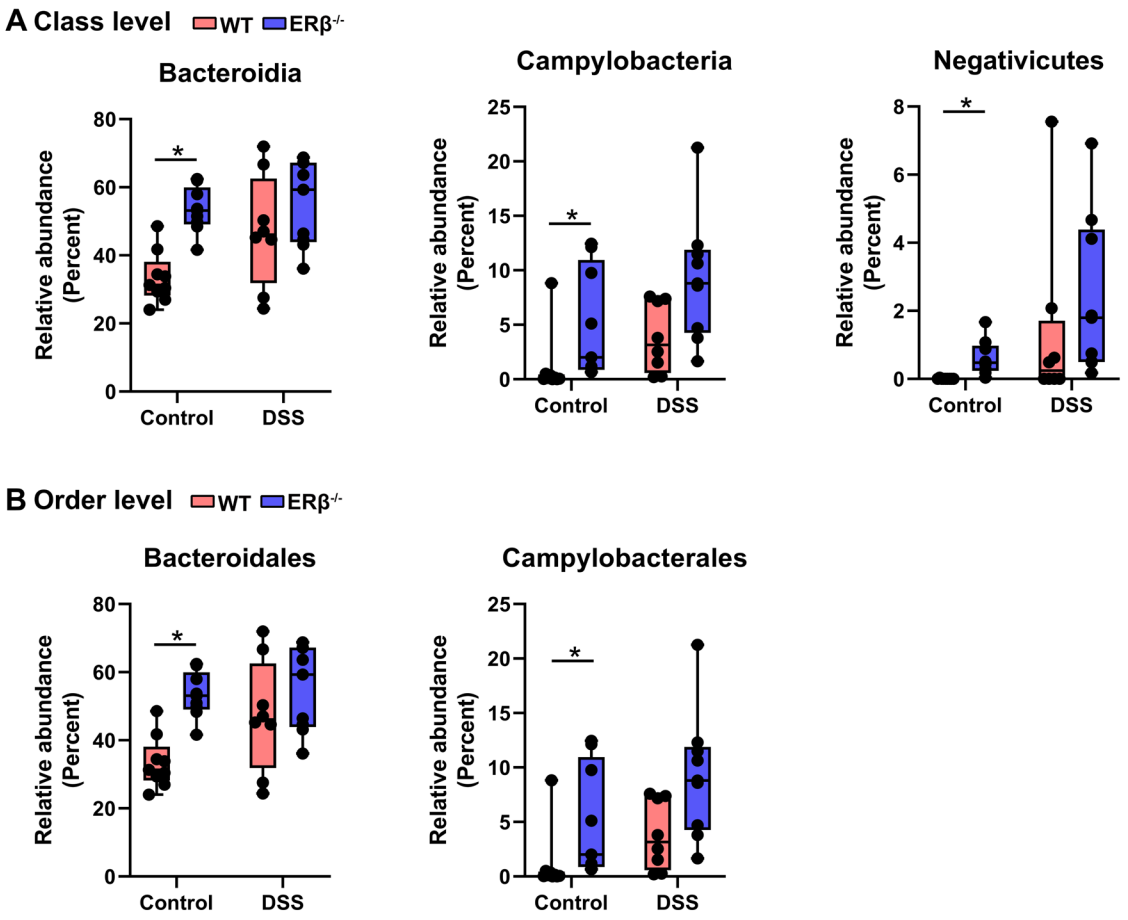

Figure S2. Fecal microbiota of WT and ERβ$^{-/-}$ mice under basal and inflammatory states in class and order levels.

(A) Relative abundances of substantially changed bacteria taxa in class level. **(B)** Relative abundances of substantially changed bacteria taxa in order level. Data are presented as boxplots. Statistical comparison was performed by non-parametric Wilcoxon rank sum. n=9/group, except for n=8 in WT DSS group. *P<0.05.

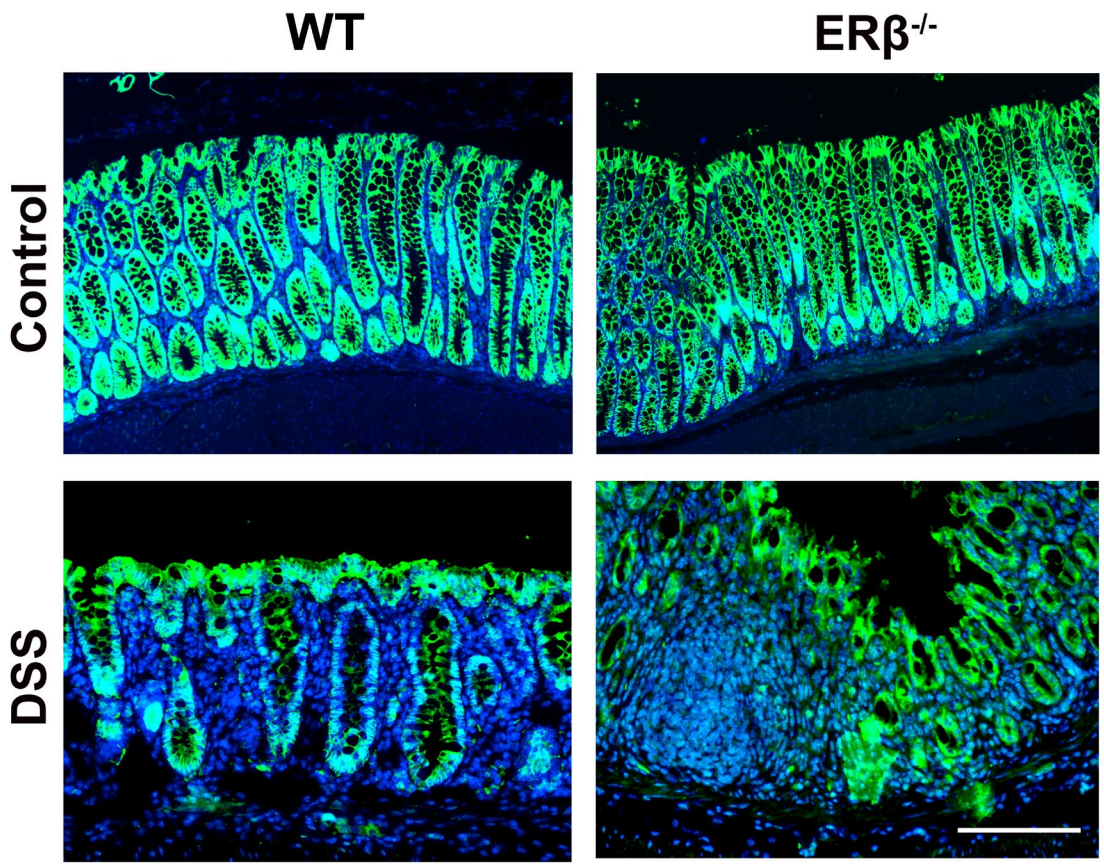

Figure S3. The tight junction in WT and ERβ$^{-/-}$ mice under basal and inflammatory states.

Representative images of Claudin1 immunofluorescence staining in distal colon of WT and ERβ$^{-/-}$ mice under homeostatic and day 5 following DSS treatment.

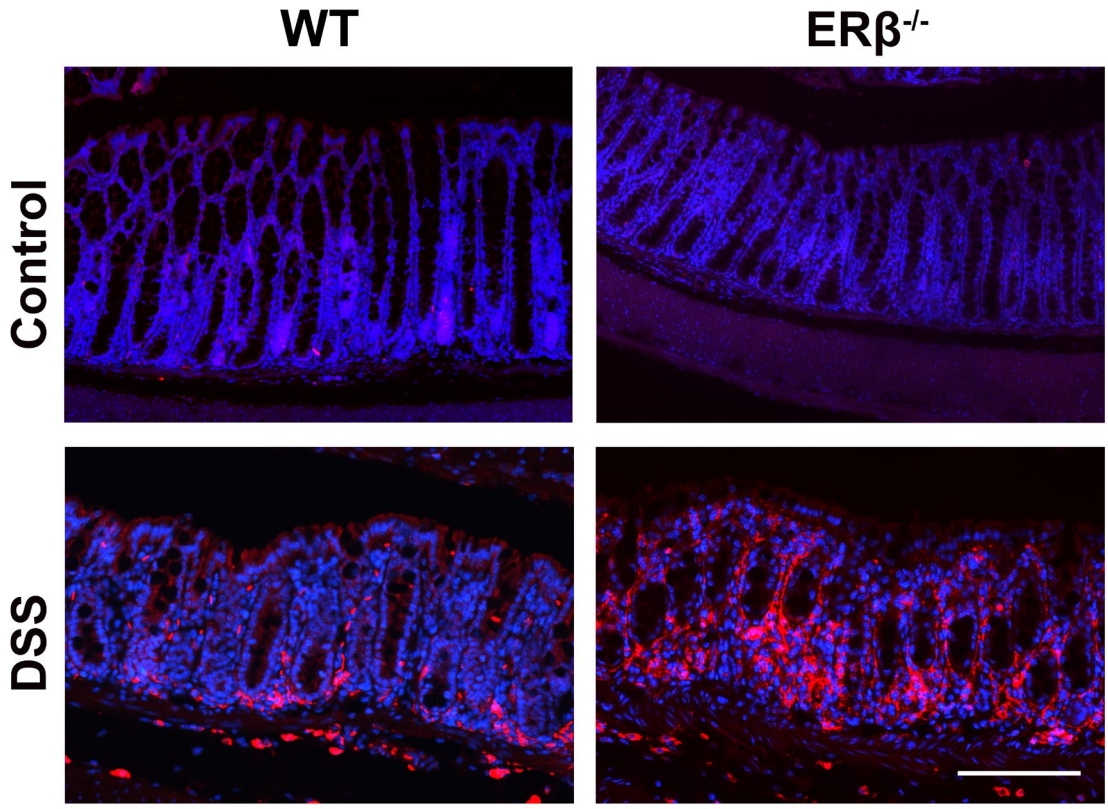

Figure S4. Aggravated macrophage infiltration in ERβ$^{-/-}$ mice treated with DSS.

Representative images of F4/80 immunofluorescence staining in distal colon of WT and ERβ$^{-/-}$ mice under homeostatic and day 5 following DSS treatment.

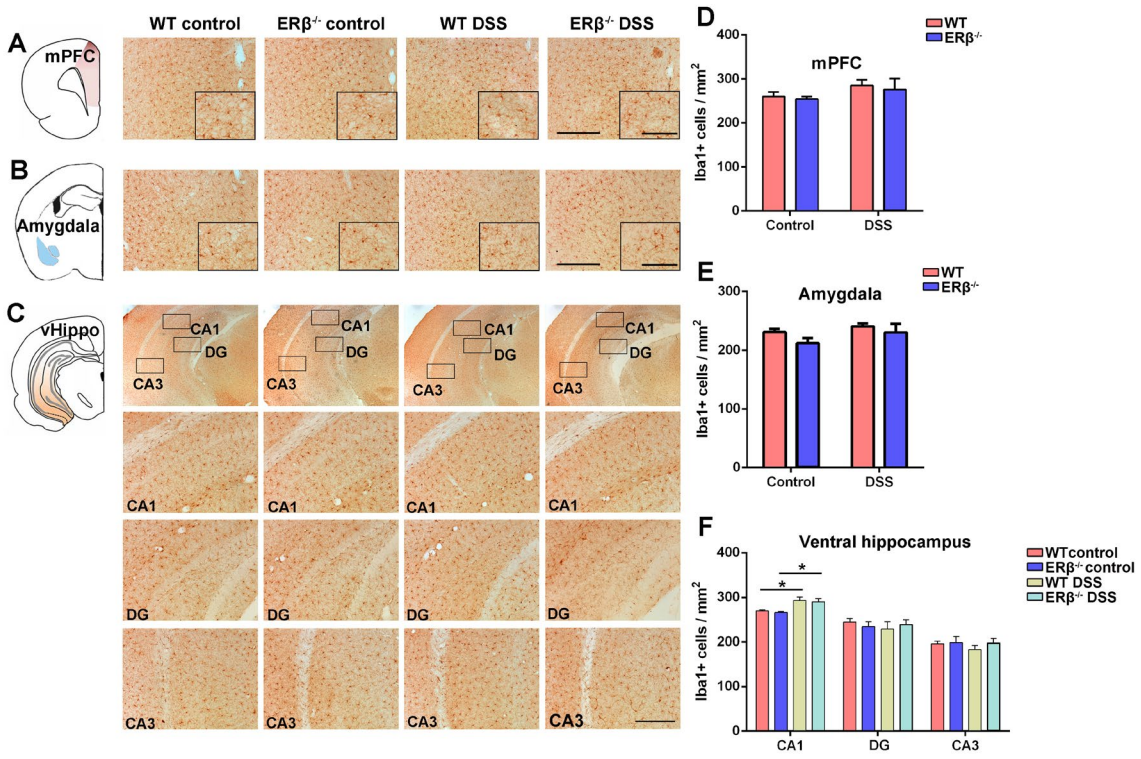

Figure S5. ERβ deficiency did not significantly influence the neuroinflammation status compared with WT mice after treated with DSS.

(A-C) Diagrams of mPFC, amygdala and ventral hippocampus, and representative images of Iba1 immunochemistry staining within mPFC (A), amygdala (B) and ventral hippocampus (C). **(D-F)** Quantitative analysis of Iba1 positive cells in mPFC (D), amygdala (E) and ventral hippocampus (including CA1, DG, CA3 areas) (F). n=4/group. Data are presented as mean ± SEM. Statistical comparison was performed by two-way ANOVA. **P*<0.05.

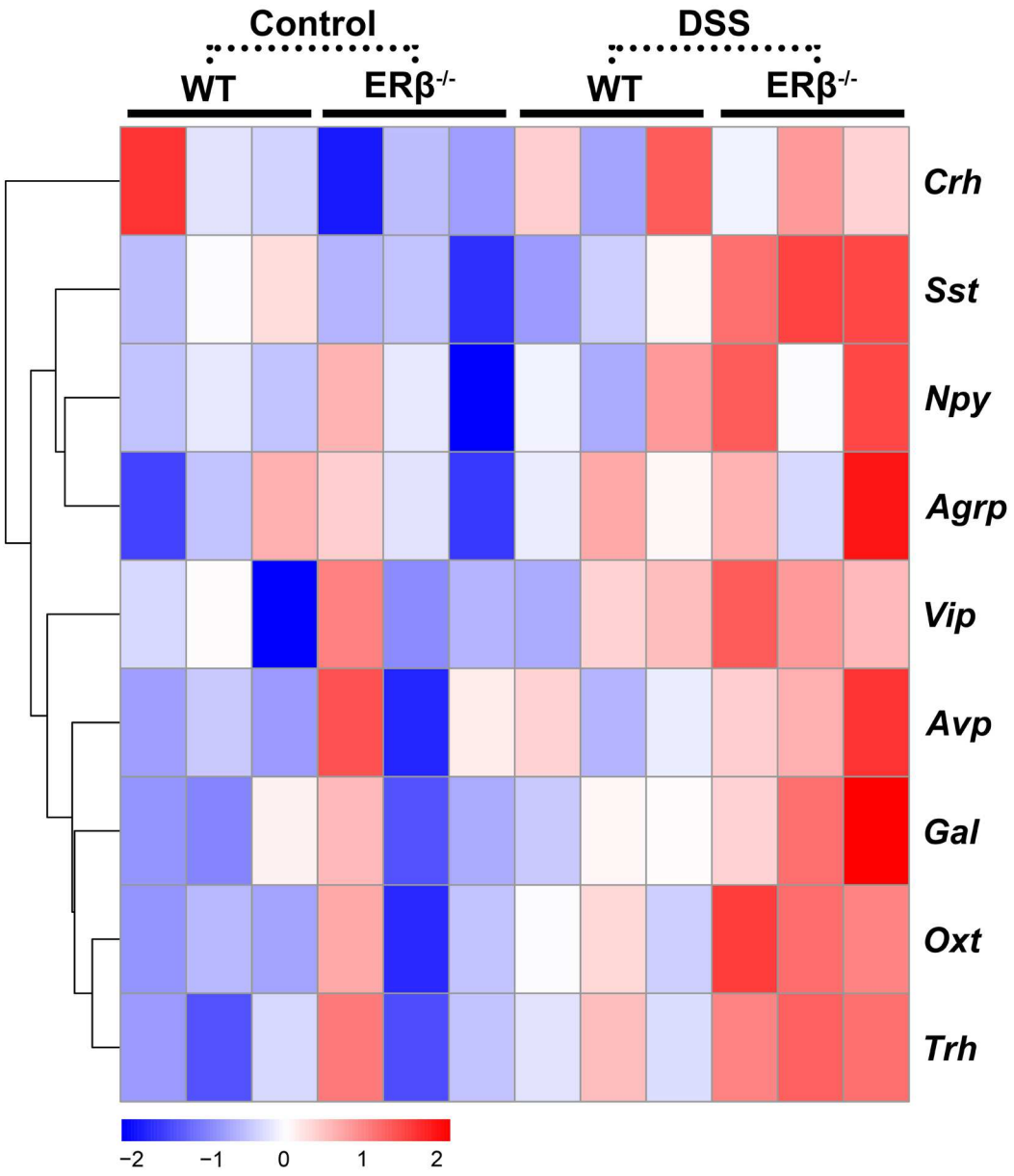

Figure S6. mRNA expressions of hypothalamic neuropeptides in ERβ$^{-/-}$ mice treated with DSS.

Hierarchical clustering heatmap of several hypothalamic neuropeptide gene expression profile (*Crh*, *Sst*, *Npy*, *Agrp*, *Vip*, *Avp*, *Gal*, *Oxt* and *Trh*) of WT and ERβ$^{-/-}$ mice under homeostasis status and treated with DSS. n=3/group.

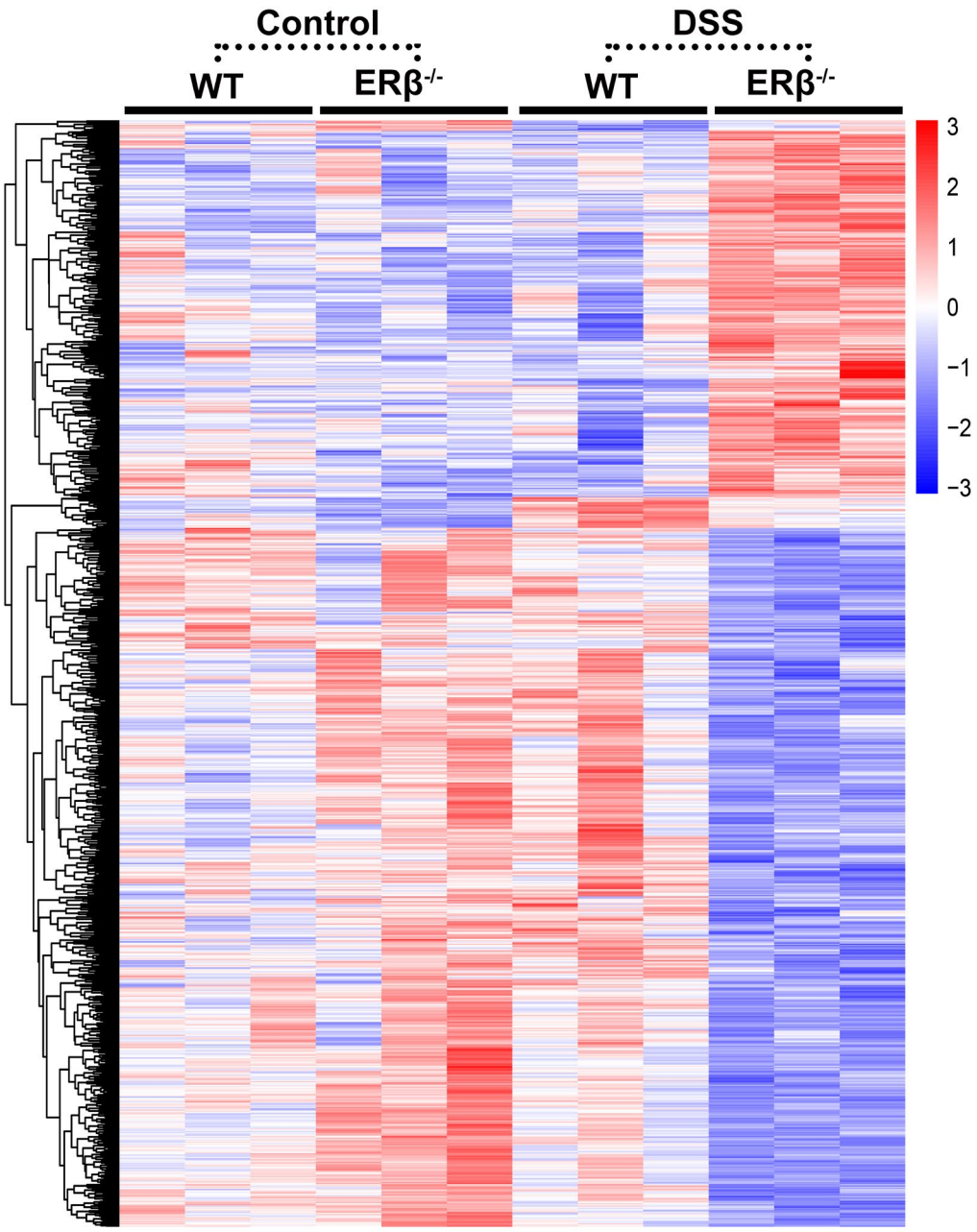

Figure S7. Hierarchical clustering of the overlapping 934 genes.

The gene expression profile of the overlapping 934 genes in hypothalamus of WT and ERβ-/- mice under homeostasis status and treated with DSS.

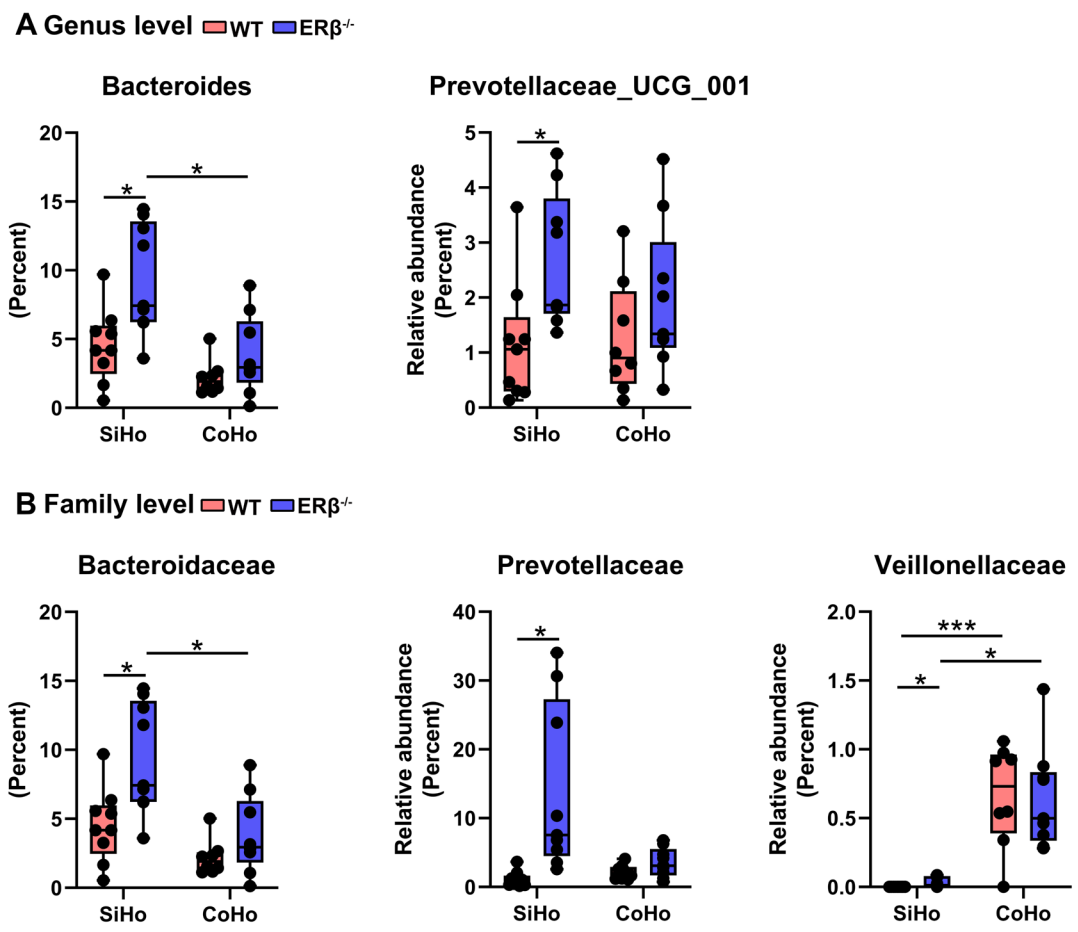

Figure S8. Fecal microbiota of SiHo WT, SiHo ERβ$^{-/-}$, CoHo WT and CoHo ERβ$^{-/-}$ mice before treated with DSS.

(A) Relative abundances of substantially changed bacteria taxa in genus level. **(B)** Relative abundances of substantially changed bacteria taxa in family level. Data are presented as boxplots. Statistical comparison was performed by non-parametric Wilcoxon rank sum. n=9/group, except for n=8 in CoHo WT group. *P<0.05, ***P<0.001.

Supplemental materials and methods

Behavioral assays

Behavioral tests were performed during day 6 to day 10 following DSS exposure and scheduled in order to avoid carry-over effects from prior testing experience.

Open field

The open field test was performed in the apparatus (40 cm × 40 cm × 30 cm) made of grey plexiglas. Initially placed in the center zone, the mouse then got access to exploring the whole arena. Noldus Observer software (Ethovision 11.0) was utilized to analyze the total distance traveled, time spent in the center zone and entries to center during the 10-min period.

Elevated plus-maze

Elevated plus-maze apparatus comprised 2 open arms (30 cm × 6 cm × 15 cm), 2 closed arms (30 cm × 6 cm × 15 cm) and a central area. Each mouse was allowed to explore the apparatus freely for 10 min with being placed facing to an open arm initially in the central zone. When 4 paws of the mouse were within the arm, the mouse was seen entirely entering the arm. The time spent in the open arms and number of entries to the open arms were analyzed by Noldus Observer software (Ethovision 11.0).

Light-dark transitions

The light-dark box comprised 2 rectangular chambers (light box: length 27 cm, width 27 cm and height 30 cm; dark box: length 18 cm, width 27 cm and height 30 cm) [1]. The mouse was placed in the bright chamber with its back to the opening and allowed to explore

the whole box freely for 10 min. The time spent in the dark side and total number of side transitions were recorded using Noldus Observer software (Ethovision 11.0).

Tail suspension test

The mice were singly suspended by a tape stuck 1 cm to the tip of the tail and 50 cm height above the ground. The duration of immobility in the last 4 min of the 6-min test was recorded.

Forced swimming test

Each mouse was individually placed in a water tank (20 cm height × 14 cm diameter) containing 10 cm of water at 25 °C for 6 min. The floating time, during which the mouse only kept inactive with its head on the surface and slight movements, was recorded to determine the duration of immobility in the last 4 min.

Nest building

Each mouse was placed in an individual home cage with a piece of cotton pads (2.5 g/5 cm^2) (Ancare, Bellmore, NY, USA). Scores were defined according to the amount of torn cotton pads and shape of the nest [2].

Y maze

Y maze apparatus comprised 3 arms (40 cm × 9 cm × 16 cm). Each mouse was allowed to explore the apparatus freely for 8 min with being placed in the central zone of Y maze. The spontaneous alteration was calculated as: number of triads containing entries into all 3 arms/maximum possible alternations (the total number of arms entered - 2) × 100% [3].

Novel object recognition

The test was performed in the open-field apparatus (40 cm × 40 cm × 30 cm). Firstly, mice were placed in the open and empty field for 30 min in the habituation period. Twenty-four hours after habituation, 2 identical objects were placed in the open field and mice were allowed to explore the objects for 10 min. After a 2 hours interval, 1 novel object was used to replace 1 object that used during habituation period, and mice were placed in the open field to explore the novel or familiar object for 10 min. The discrimination index was calculated as: time exploring novel object/(time exploring novel object + time exploring familiar object) × 100%.

Three chamber test

The three chamber test was performed in a rectangular socialization apparatus (60 cm × 40 cm × 22 cm) with 3 chambers as previously described [4]. Firstly, each mouse was place in the middle chamber and allowed to explore the apparatus freely for 10 min during the habituation period. In the social approach period, an unfamiliar C57BL/6 male mouse (novel mouse) was placed in one side of the apparatus, and a novel object was placed in the opposite side. Then, the tested mouse was allowed to explore the apparatus for 10 min. In the social novelty period, another unfamiliar C57BL/6 male mouse (novel mouse) was placed in one side of the apparatus, and the mouse that used in the social approach period (familiar mouse) was placed in the opposite side. Next, each mouse was placed in the apparatus to explore the box for 10 min. The time in each chamber and sniffing time for mouse or object were recorded using Noldus Observer software (Ethovision 11.0).

16S rRNA gene sequencing and data analysis

Total microbial genomic DNA were extracted from mouse fecal pellets by DNeasy PowerSoil Kit (QIAGEN) and V3-V4 regions of bacterial 16S rRNA genes were PCR

amplified using modified universal primer pairs. After PCR reaction in triplicate, Agencourt AMPure Beads (Beckman Coulter) was utilized to purify PCR amplicons, followed by quantification using the PicoGreen dsDNA Assay Kit (Invitrogen). Based upon the Illumina MiSeq platform, paired-end 2×300 bp sequencing was performed with MiSeq Reagent Kit. Sequence data were processed by open reference OTU picking, which shared 97% sequence similarity to the SILVA132 database, then analyzed by QIIME and R packages (v3.2.0).

Histopathology

Colonic and hypothalamic tissues were fixed in 4% paraformaldehyde (PFA)/PBS overnight and embedded in paraffin. The samples were cut into 5 μm. The degree of colonic injury was coded and assessed in a blinded fashion by hematoxylin and eosin (HE) and alcian-blue periodic acid schiff (AB-PAS) staining colonic sections based on a scale that grades the extent of inflammatory infiltration (0–5), ulceration (0–3) and crypt damage (0–4) [5]. The detailed scoring system for histological changes in the colon were presented in Table S1.

Quantitative real-time PCR

Total RNA of colon and hypothalamic tissues was extracted using an Ultrapure RNA kit (CWBIO), which of qualified concentration was reverse transcribed into cDNA following the instructions of the PrimeScript RT Reagent Kit (Takara). The qRT-PCR was carried out and analyzed by the CFX96 Real-Time PCR system (Bio-Rad). The experiments were carried out in triplicate and the averaged relative levels of target mRNAs were normalized to GAPDH expression level. The primer sequences used are listed in Table S2.

Immunohistochemistry

Paraffin sections were processed for antigen retrieval as our previous method [4], and incubated with primary antibodies in 1% bovine serum albumin (BSA) overnight at room temperature. Colonic sections were incubated with anti-Claudin1 (Invitrogen) and anti-F4/80 (Biolegend) antibodies, and hypothalamic sections were incubated with ionized calcium binding adapter molecule 1 (Iba1) (Dako), anti-corticotropin releasing hormone (Crh) (Sigma-Aldrich), anti-arginine vasopressin (Avp) (Santa Cruz Biotechnology), anti-oxytocin (Oxt) (Chemicon) and anti-ErbB4 (Invitrogen). For immunohistochemistry staining, sections were incubated with corresponding secondary antibody (1:200, room temperature), followed by incubation with the avidin-biotin-peroxidase complex and 3,3-diaminobenzidine tetrahydrochloride as the chromogen. For immunofluorescence staining, sections were incubated with 488- or Cy3-conjugated secondary antibodies (1:500, room temperature) and then treated with 4', 6-diamidino-2-phenylindole (DAPI, Sigma-Aldrich). The images were captured by Zeiss microscope and Axiocam HR camera using Axiovision software (both Carl Zeiss) at 20× magnification.

Paraventricular nucleus (PVN) of hypothalamus was selected for analysis and identified using a standard mouse brain atlas [6]. Crh^+, Avp^+, Oxt^+ and $ErbB4^+$ cells were manually counted bilaterally in 3 representative brain sections per mouse and normalized to the size of area.

Enzyme linked immunosorbent assays

To determine corticosterone and adrenocorticotropic (ACTH) hormone levels, trunk blood was collected in EDTA coated eppendorf tubes following rapidly decapitated under isoflurane anesthesia from mice. Next, after spinned for 10 min at 4 °C, the serum was

collected and stored at -80°C until processing. Corticosterone and ACTH levels were determined by Elisa kits (Enzo) following manufacturers' guidelines.

RNA sequencing

RNA was extracted from hypothalamus by RNeasy Plus Micro kit (Qiagen). The sequencing libraries were generated using NEBNext Ultra RNA Library Prep Kit for Illumina, then were pooled and sequenced on Illumina NovaSeq 6000 platforms with paired-end 150-bp sequencing. Raw reads with low-quality bases (N>10%) and adaptor contaminants were removed, and the clean reads were aligned to the mouse reference genome (mm10) using TopHat v2.0.12. Gene count expression level was analyzed by HTSeq v0.6.1, and next differentially expressed transcripts and genes were analyzed by using the DESeq R package (1.18.0). Genes with *P* values <0.05 were set as significantly differential expression. KOBAS software was used to test the statistical enrichment of differential expression genes in KEGG pathways between groups.

Data availability

Original transcript profiling and 16S rRNA sequencing data were deposited at the NCBI Sequence Read Archive (SRA) under the accession number PRJNA632986.

References

1. Babri S, Doosti MH, Salari AA. Strain-dependent effects of prenatal maternal immune activation on anxiety- and depression-like behaviors in offspring. Brain Behav Immun. 2014; 37:164-76.
2. Deacon RM. Assessing nest building in mice. Nat Protoc. 2006; 1(3):1117-1119.

3. Zhong H, Xiao R, Ruan R, Liu H, Li X, Cai Y et al. Neonatal curcumin treatment restores hippocampal neurogenesis and improves autism-related behaviors in a mouse model of autism. Psychopharmacology. 2020; 237(12):3539-52.
4. Cai Y, Tang X, Chen X, Li X, Wang Y, Bao X et al. Liver X receptor beta regulates the development of the dentate gyrus and autistic-like behavior in the mouse. Proc Natl Acad Sci U S A. 2018; 115(12):E2725-33.
5. Xu J, Zhou L, Ji L, Chen F, Fortmann K, Zhang K et al. The REGgamma-proteasome forms a regulatory circuit with IkappaBvarepsilon and NFkappaB in experimental colitis. Nat Commun. 2016; 7:10761.
6. Franklin K, Paxinos G, Keith B. The mouse brain in stereotaxic coordinates. 2008; 3(2):6.

Supplemental tables

Table S1. Scoring system for histological changes in the colon.

Score	Inflammatory infiltration	Ulceration	Crypt damage
0	No infiltrate	None	None
1	Occasional cell limited to lamina propria	Small, focal ulcers	Some crypt damage, spaces between crypts
2	Significant presence of inflammatory cells in lamina propria, limited to focal areas	Frequent small ulcers	Larger spaces between crypts, loss of goblet cells, some shortening of crypts
3	Infiltrate present in both submucosa and lamina propria, limited to focal areas	Large areas lacking surface epithelium	Large areas without crypts, surrounded by normal crypts
4	Large amount of infiltrate in submucosa, lamina propria and surrounding blood vessels, covering large areas of mucosa		No crypts
5	Transmural inflammation		

Table S2. The sequences of primers used in this study.

Gene	Primer sense (5'-3')	Primer antisense (5'-3')
Tnfa	GATCGGTCCCCAAAGGGATG	TGAGGGTCTGGGCCATAGAA
Il1b	TGCCACCTTTTGACAGTGATG	AAGGTCCACGGGAAAGACAC
Il6	GGAGCCCACCAAGAACGATAG	GTGAAGTAGGGAAGGCCGTG
Il17a	TGATCAGGACGCGCAAACAT	GGTCTTCATTGCGGTGGAGAGT
Cxcl1	GGTGTCCCCAAGTAACGGAG	TTGTCAGAAGCCAGCGTTCA
Ifng	CGGCACAGTCATTGAAAGCC	TGTCACCATCCTTTTGCCAGT
Erbb4	GCTCGCAAGTGGCTATGGTA	TCGCCAGCTTCATTTTTGGC
Pik3ca	ATGCCCCCACGAATCCTAGT	GAGGGTATTTCCTGGCCTCTC
Pik3r1	GTGCGGGCCGTATAGGTTTTA	TGCGACAGTTTCCTTGGCTT
Akt2	GGTTCGAGAGAAGGCCACTG	GGAAGGGGTGCCTGGTATTC
Gsk3b	CCCTTCTGTTCGGCTACCTT	AAGCCGGAACCAATCAGAGA
Cdkn1a	GCAGATCCACAGCGATATCCA	GACAACGGCACACTTTGCTC
Gapdh	TGGGTGTGAACCACGAGAAA	AAAGTTGTCATGGATGACCTTGG